THE UNIVERSITY OF QUEENSLAND

Bachelor of Engineering Thesis

Design of a load dissipation device for a 100kW
supercritical CO2 turbine

Student Name: Mitchell LOWE

Course Code: MECH4500

Supervisor: Mr Hugh Russell

Submission date: 28 October 2016

A thesis submitted in partial fulfilment of the requirements of the
Bachelor of Engineering degree in Mechanical Engineering

UQ Engineering

Faculty of Engineering, Architecture and Information Technology

ACKNOWLEDGEMENTS

I would firstly like to extend my gratitude to Hugh Russell. Completing this thesis has given me a great deal of satisfaction and I am proud of the work that I have produced. Thank you for providing me with this opportunity.

To Joshua Keep, your knowledge, experience and passion in the field of turbomachinery has made working under your supervision an enjoyable experience. Thank you for your encouragement and patience over this year and all the best for your continued studies.

ABSTRACT

The Queensland Geothermal Energy Centre of Excellence (QGECE) require a load dissipating device in order to conduct tests in isolation on supercritical CO_2 turbines. The turbines of interest are to be designed by QGECE to produce 100kW of power while rotating at 120kRPM. A device that is able to meet these requirements is presented in this thesis in the form of a centrifugal compressor.

To establish the aerodynamic design of the centrifugal compressor, a 1-Dimensional mean-line analysis method was adapted into a Python code. Mean line analysis techniques are typically employed when establishing the preliminary geometry of a centrifugal compressor that is required to meet a set of design constraints for a new application. Further to nominal design, it is also typical to quantify off-design performance at anticipation points of operation. To do this, NASA's FORTRAN model for predicting the off-design performance for centrifugal compressors was adapted into a Python code.

Both the geometry and off-design codes were validated by comparison of the published performance and dimensions of an off-the-shelf centrifugal compressor. The code was then used to design a compressor for an operating point of 0.4kg/s of mass flow and a pressure ratio of 4.8, which were the calculated performance constraints required to dissipate 100kW of power at 120kRPM. These constraints were determined based on the material and exducer radius selected for the impeller design. The impeller was the key component to be designed as it provides the energy responsible for the compression. Because of this, the housing and diffuser could be adapted from an off-the-shelf turbocharger.

The final design features a 40° backswept machined titanium alloy impeller with a 105mm exducer and a 55mm inducer. The titanium alloy selected for the impeller was Ti-6242, based on its high strength and superior machinability in comparison to other titanium alloys used in turbomachinery design. The small inducer and large exducer are features that are typical of a low mass flow, high pressure ratio centrifugal compressor. As efficiency was not a key consideration in the design and cost was to be minimised, a modified off-the-shelf housing taken from a GT4508R turbocharger manufactured by Garrett was implemented.

At a mass flow rate of 0.292kg/s and pressure ratio of 6.4, the design was shown to dissipate 100kW of power at 120kRPM. Despite a demonstration of the design's ability to meet the requirements, a CFD analysis was recommended to increase the validity of the demonstration before procurement.

The load dissipation device presented in this thesis in the form of a centrifugal compressor will allow QGECE to conduct tests and demonstrate their capability to design supercritical CO_2 turbines.

CONTENTS

LIST OF FIGURES

LIST OF TABLES

NOMENCLATURE

Variables

Table 1: Nomenclature for the variables used in this thesis

Variable	Meaning	Units
$W_{c,s}$	Compressor isentropic work	W
$\dot{m}$	Mass flow rate	kg/s
h	Enthalpy	kJ/kg
C_p	Specific heat at constant pressure	kJ/kgK
T	Temperature	K
s	Entropy	kJ/kgK
P	Pressure	Pa
γ	Ratio of specific heats	-
η_{isen}	Isentropic efficiency	%
$\Pr(i)$	Pressure ratio (Iterated)	-
MFP	Mass Flow Parameter	kg/s K$^{1/2}$/MPa
SP	Specific Speed	rps/K$^{1/2}$
U	Blade tangential velocity	m/s
V	Absolute fluid velocity	m/s
W	Relative fluid velocity	m/s
r	Radius	M
τ	Torque	N.m
C	Absolute fluid velocity	m/s
ρ	Density	kg/m^3
A	Area	m^2
β	Relative angle	°
α	Absolute angle	°
λ	Swirl parameter	-
CpD	Diffuser static pressure recovery coefficient	-
Z	Number of blades	-
N	Shaft rotational speed	kRPM

Variable	Meaning	Units
AR	Area ratio of the diffuser	-
σ	Slip factor	-
σ'	Stress	MPa
v	Poisson's ratio	-
ω	Shaft rotational speed	rad/s
k	Thermal conductivity	Btu/(h ft °F)
E	Young's modulus	MPa
H_B	Birnell Hardness number	-

Note: k is used in the codes of the appendix to describe the ratio of specific heats however in the report it is used for the thermal conductivity of materials

Subscripts

Table 2: Nomenclature for the subscripts used in this thesis

Subscript	Meaning
0	Stagnation property, upstream of inducer
1	Inducer property
2	Exducer property
3	Diffuer exit property
b	Blade property
m	Meridional direction, mixed out property
D	Diffuser property
i	Ideal property
x	Specific property
θ	Tangential direction
t	Tip property
h	Hub property
s	Isentropic

Note: multiple subscripts may be used for the one variable. For example, T_{02m} is the stagnation temperature at the exducer and it is a mixed out property

1 INTRODUCTION

1.1 Background

One of the key research areas conducted by the Queensland Geothermal Centre of Excellence (QGCEC) is the development of supercritical turbines for Brayton cycles, with Carbon Dioxide (CO_2) as the working fluid. These turbines are tested using an isolated power cycle in Pinjarra Hills, Brisbane. In order to test the power output of the turbine in isolation, a device is needed to dissipate and measure the turbine shaft power.

Currently, the test facility is operating with Pentafluoropropane (r245fa) as the working fluid at sub-critical conditions. The turbine shaft of this cycle produces a small power output (7kW) and rotates at relatively slow speeds (30krpm). A water-brake dynamometer is used to dissipate and measure the power output.

QGECE are interested in testing supercritical Carbon Dioxide (sCO_2) in the cycle which will produce higher power outputs and faster turbine shaft speeds. There are no off-the-shelf water brake dynamometers that can withstand the high rotational speeds and resultant power. For testing the power output up to 20kW, at 120kRPM shaft speed, a centrifugal compressor adapted from a turbocharger is currently undergoing development. The turbocharger is manufactured by Holset.

Future testing by QGECE requires a device that is capable of dissipating 100kW of power at a rotational speed of 120kRPM. A centrifugal compressor is a logical option for this application as the rotational speed and power output from the turbine exceeds the limitations of other devices such as dynamometers and gearboxes. Currently, there are no appropriate centrifugal compressors available to QGECE that can dissipate 100kW at 120kRPM. This is due to speed limited and stress limited constraints. The aim of this thesis is to propose a solution to these requirements.

The overall structure of this thesis is as follows:

- *Chapter 1* outlines the objectives, scope and definition of the problem that this thesis aims to address;

- *Chapter 2* discusses relevant literature and identifies possible solution paths to the design problem;

- *Chapter 3* assesses the feasibility of the potential design options found in literature;

- *Chapter 4* outlines the methodology used to design the load dissipation device;

- *Chapter 5* presents the final design and demonstrates its ability to meet the requirements;

- *Chapter 6* presents the conclusions and recommendations.

1.2 Objectives

The objective of the thesis is to:

- Propose an architecture for the load dissipation device.

- Propose a detailed design of an architecture that can dissipate 100kW of power at 120kRPM.

- Propose a Bill of Materials to accompany the detailed design.

The significance of this work is that it will allow QGECE to conduct tests and demonstrate their capability in designing supercritical CO_2 turbines.

1.3 Scope

Table 3 summarises the scope of work of this study.

Table 3: Thesis scope

In scope	Out of scope
- Preliminary aerodynamic design of a centrifugal compressor impeller using 1-Dimensional mean line analysis - Off-design performance analysis using 1-Dimensional mean line methods. - Validation of analysis using published geometry and performance of a commercially manufactured centrifugal compressor - Demonstration of the final design's ability to meet the design requirements. - Consideration of alternative design options - Selection of the working fluid and materials required to meet the design constraints - A cost estimate of the final design with a Bill of Materials	- Detailed aerodynamic modelling using Computational Fluid Dynamics (CFD) - Secondary and mixed flow calculations - Mechanical design of ancillary components such as shafts and bearings - Determination of aerodynamic thrust loading from the impeller

1.4 Problem definition and theory

The performance of compressors is typically characterised by compressor maps produced by the manufacturer. Compressor maps are used to match the pressure and mass flow rate required for a particular application to a specific model of compressor. *Figure 1* is an example of compressor map from Holset. The vertical axis shows the total-to-total pressure ratio between the inlet and outlet of the compressor. The horizontal axis shows the normalised mass flow (see *Equation 7*). The graph is bounded left to right by the phenomena of surge and choke respectively (discussed in *Section 2.1*). The graph is bounded top to bottom by maximum and minimum normalised operating speeds of the compressor (see *Equation 8*). The contour lines between these bounds indicate the efficiency.
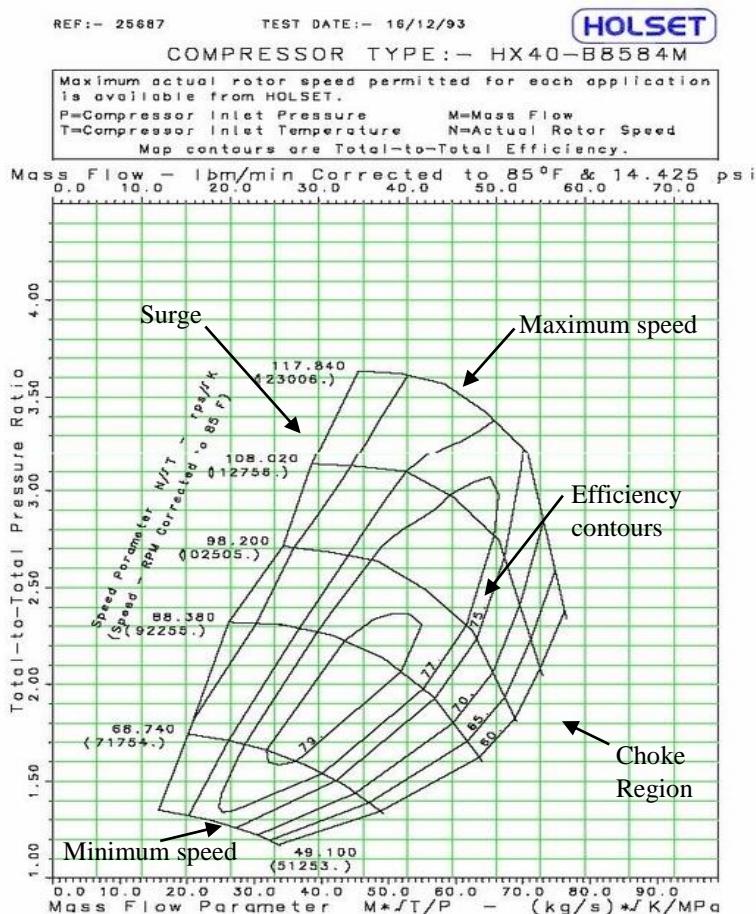
Figure 1- Compressor map of model HX40-B8584M from Holset

For the purpose of power dissipation, an expression for, pressure ratio as a function of mass flow rate and power, is required. This expression is referred to in this thesis as the line of constant power. By superimposing the line of constant power on top of a compressor map, the pressure ratio and mass flow rate at which a constant level of power is dissipated can be established. The intersection between the line of constant power and the normalised speed curves of the compressor map indicate an operating point for the compressor. The following section outlines the development of the expression for pressure ratio as a function of mass flow rate and power.

From the first law of thermodynamics, the isentropic work done on a fluid by a compressor can be described by *Equation 1*:

$$W_{c,s} = \dot{m}(h_2 - h_1) [1]$$

For a fluid that can be modelled as an ideal gas (such as air), the change in enthalpy is:

$$h_2 - h_1 = C_p(T_2 - T_1) [2]$$

Substituting [2] into [1] provides and expression for the isentropic work as a function of temperature:

$$W_{c,s} = \dot{m}C_p(T_2 - T_1) [3]$$

The change in entropy across the compressor is:

$$\Delta s = C_p \ln\left(\frac{T_2}{T_1}\right) - R\ln\left(\frac{P_2}{P_1}\right) [4]$$

Assuming isentropic compression, setting *Equation 4* to zero, and substituting R for the difference of specific heats give an expression for the outlet temperature as a function of the inlet temperature and pressure ratio:

$$T_2 = T_1\left(\frac{P_2}{P_1}\right)^{\frac{\gamma-1}{\gamma}} [5]$$

Where γ is the ratio of specific heats. Substituting *Equation 5* into *Equation 3*, and dividing by the isentropic efficiency of the compressor gives a function of the compressor work.

$$W_c = \frac{\dot{m}C_pT_1\left((Pr)^{\frac{\gamma-1}{\gamma}} - 1\right)}{\eta_{isen}} [6]$$

The compressor maps are typically shown with a normalised flow rate on the x-axis and pressure ratio on the y-axis. The mass flow rate is normalised to remove the influence of ambient testing conditions (Keep, 2016). For the same purpose, some manufacturers normalise the rotational speed for the compressor shaft. These normalisations of compressor flow are not standardised across industry. For the purposes of demonstrating the matching process, the normalisation equations for mass flow rate and shaft speed used by the manufacturer Holset are utilised. Their equations were chosen as a Holset compressor is currently being development for the 20kW requirement. The mass flow parameter (MFP) plotted on the x-axis is described by:

$$MFP = \frac{\dot{m}\sqrt{T_1}}{P_{atm}[MPa]} [7] \qquad \text{MPa??}$$

Where atmospheric pressure is in units of mega-pascals. The speed parameter (SP) is described by:

$$SP = \frac{N}{\sqrt{T_1}} \ [8]$$

Where N is the rotational speed in units of revolution per second and temperature is in Kelvin. Combining *Equation 6* and *Equation 7* and rearranging for pressure ratio gives an equation that can be used compare compressor requirements to manufacturer compressor maps:

$$\text{Pr} = \left[\frac{\eta_{isen} W_c}{P_{atm} MFP C_p \sqrt{T_1}} + 1 \right]^{\frac{\gamma}{\gamma-1}} [9]$$

Equation 9 was plotted in *Figure 2* for 20kW and 100kW using the python script found in *Appendix 8.1*. The properties of air at atmospheric conditions were used as the inlet properties in *Equation 8* (0.1013MPa, 298K). The ratio of specific heats at these conditions is 1.4 and the specific heat at constant pressure of 1006 J/kg. An isentropic efficiency of 75% was assigned to the compressor as an initial assumption recommended by QGECE.

Figure 2 below demonstrates the matching of the Holset compressor map for the HE351ve model turbocharger which has been adapted by QGECE and is undergoing development for the dissipation of 20kW of power. The points on the map shown below were extracted from the original compressor map. The intersection of the requirement lines with the speed curves of the compressor map represent the operating points for the compressor, which are marked with an "X."
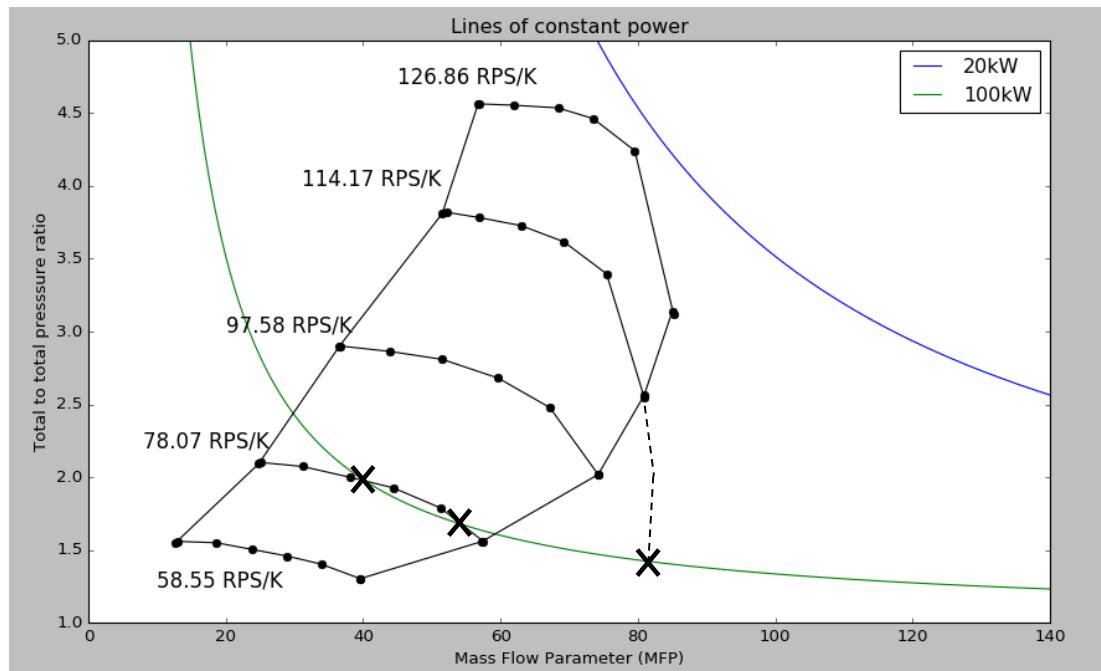
Figure 2: 20kW and 100kW requirement superimposed over Holset compressor map

Note that the efficiency contours are not shown on this plot. It must also be noted that typically, manufactures only present compressor maps down to the 60% efficiency contour (as shown in the

example map in *Figure 1*). This is because lower values are of no interest for internal combustion engine applications (Keep, 2016). Because the key requirement of the design is dissipating power at high speed, the efficiency of the compressor is not an important design requirement which allows the speed curves to be extrapolated further into the choke region. As the speed curves move further into a region of lower efficiency, they begin to asymptote (R.Flemming, 2011). At 120kRPM, the normalised speed is 115.85rps/K (calculated using *Equation 8*) which can be closely approximated by the 114.17rps/K speed curve shown on the map. The dotted line shows this extrapolation, and highlights the intersection of 120kRPM with the 20kW requirement line.

Additionally, the plot shows that the 100kW line does not intersect any of the speed curves. This highlights the problem this thesis topic aims to address. It is obvious that the 100kW requirement does not match the compressor model used for the 20kW requirement. Based on this problem definition, and by observing *Equation 8*, there are three options to investigate in order to design a load dissipation device for the 100kW requirement:

1. Undertake a further search into commercially available compressors designs that could meet the design requirements

2. Custom design a compressor to meet the requirements

3. Control the inlet properties of the flow by:

   a. Increasing the inlet pressure and temperature

   b. Using a working fluid with a higher density and larger ratio of specific heats.

Each of these options would decrease the pressure ratio for a given MFP, shifting the line of constant power towards the bottom left of the graph and potentially into a region that intersects the speed curve for the HE351Ve compressor used for the 20kW application.

2 LITERATURE REVIEW

2.1 Aerodynamic characteristics of centrifugal compressors

A centrifugal compressor is a turbomachine that imparts energy to a continuous flow of fluid with the purpose of raising its pressure (Sorokes, 2013). A centrifugal compressor is made up of three main sections: the inducer (inlet), the impeller and the diffuser (outlet) which are highlighted in *Figure 3* (Boyce, 2006). The geometry and rotation of the impellers increases the fluids velocity and changes the flow path from the axial to the radial direction. This results in an increase in the kinetic energy of the fluid by changing its angular momentum (Japikse, 1996). The fluid exits the impeller with high velocity before being diffused. The reduction in velocity of the fluid in the diffuser converts the kinetic energy to potential energy, in the form of a static pressure rise (Sorokes, 2013).
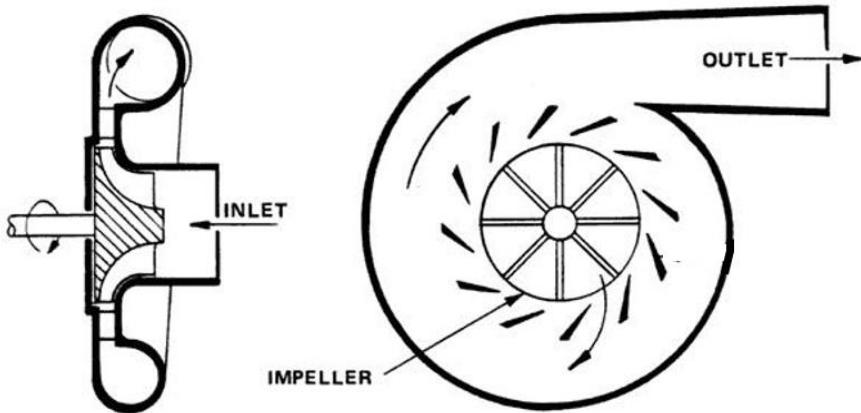
Figure 3: Basic schematic of a centrifugal compressor

The performance of centrifugal compressors is bounded by the phenomena of surge and choke. Surge is an unstable condition that occurs when the compressor cannot provide the adequate pressure rise needed to move the flow downstream (Boyce, 2006). The boundary layer of the fluid stream separates from the surface of the impeller blades, resulting in stall. The boundary layer separation reduces the passage area between two adjacent impeller blades in which the fluid can pass through. This reduction in area causes a pressure build up at the inducer that retards the incoming axial flow. This retardation of the flow changes the angle at which the fluid enters the impeller blades, causing boundary layer separation to propagate as shown in *Figure 4* (Boyce, 2006). *Figure 4* highlights the boundary layer separation, the retardation of the flow, the direction of rotation and the propagation of stall throughout the impeller.
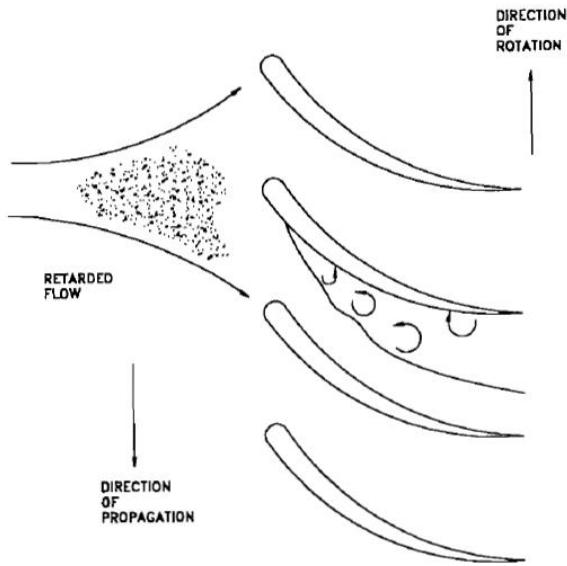
Figure 4: Propagation of stall in impeller blades of a compressor (Boyce, 2006)

The propagation of stall increases the pressure at the inducer due to the reduction of area between the blades. When this pressure build-up becomes sufficiently high, the fluid can begin to flow in the opposing direction to its normal path. The fluid moving in the opposite direction causes a build-up of pressure up stream of the inducer. This returns the compressor back to its normal operation and cycle repeats itself. This cyclic change in pressure results in erratic vibration of the housing and mechanical damage to the compressor components (Japikse, 1994).

Choke is the other bound on the performance of centrifugal compressors. If at any point throughout the compression, the flow reaches the sonic state (Mach number of 1) it is said to be choked (Japikse, 1996). Choke is the thermodynamic limit of compressible flow, where the fluid is bounded by total pressure, temperature and area (Japikse, 1994). No more mass flow can physically pass through the compressor. When the flow has an absolute velocity of Mach 1, shock waves can begin to form in the impellers which reduces efficiency and static pressure rise throughout the compressor. Shock waves can also trigger stall.

Between the bounds of surge and choke, the performance of a centrifugal compressor can be accurately calculated using 1-Dimensional mean line analysis methods. A 1-Dimensional mean line analysis considers the overall characteristics of the flow at each stage in the compressor. This is in contrast to higher levels of analysis where the internal flow phenomena are considered (Japikse, 1996). Each stage in the compressor is shown in *Figure 5*. *Figure 5* is a meridional view of a single compressor blade. A meridional view shows the mean line path of the flow through inducer, impeller and diffuser in a 2-Dimensional schematic. Each calculation stage is described in *Table 4.*
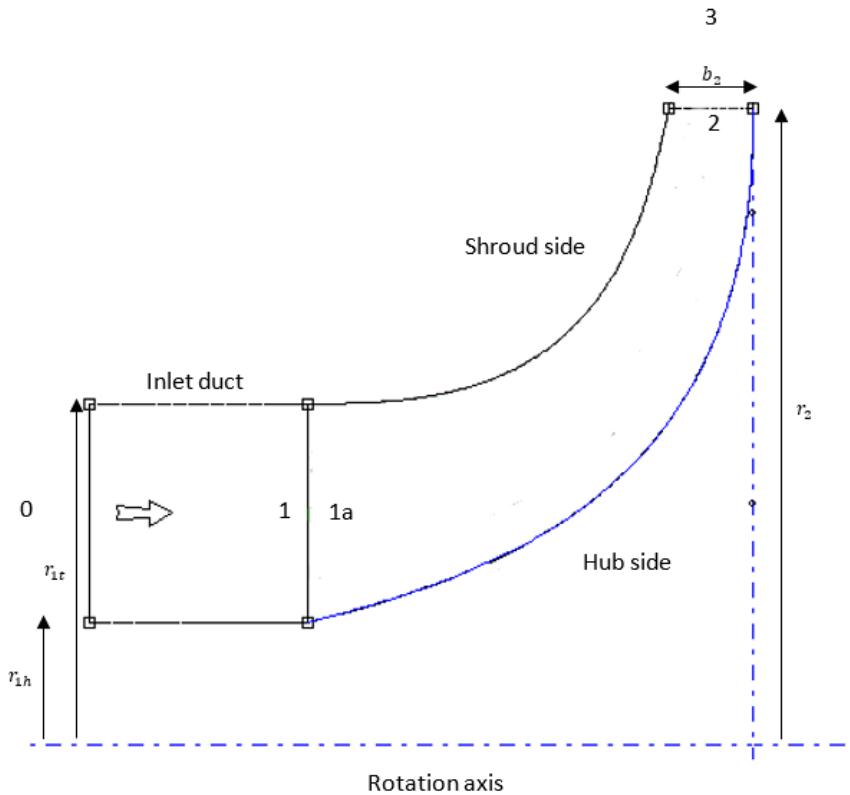
Figure 5: Meridional view of a centrifugal compressor with labelled calculation stages

Table 4: Calculation stages throughout the compressor

Stage number	Description
0	Atmospheric conditions from which the compressor is drawing air.
1	Flow properties at the inducer
1a	Flow properties just inside the impeller blades
2	Average (mixed out) flow properties at the impeller exit
3	Average (mixed out) flow properties at the diffuser exit

The properties of the flow at the inducer and outlet of the impeller (exducer) can calculated using a velocity diagram. A typical diagram for a backswept centrifugal compressor is shown in *Figure 6*. The diagram shows the velocity vectors for the inlet and outlet conditions broken into their respective radial, tangential, absolute and relative components.
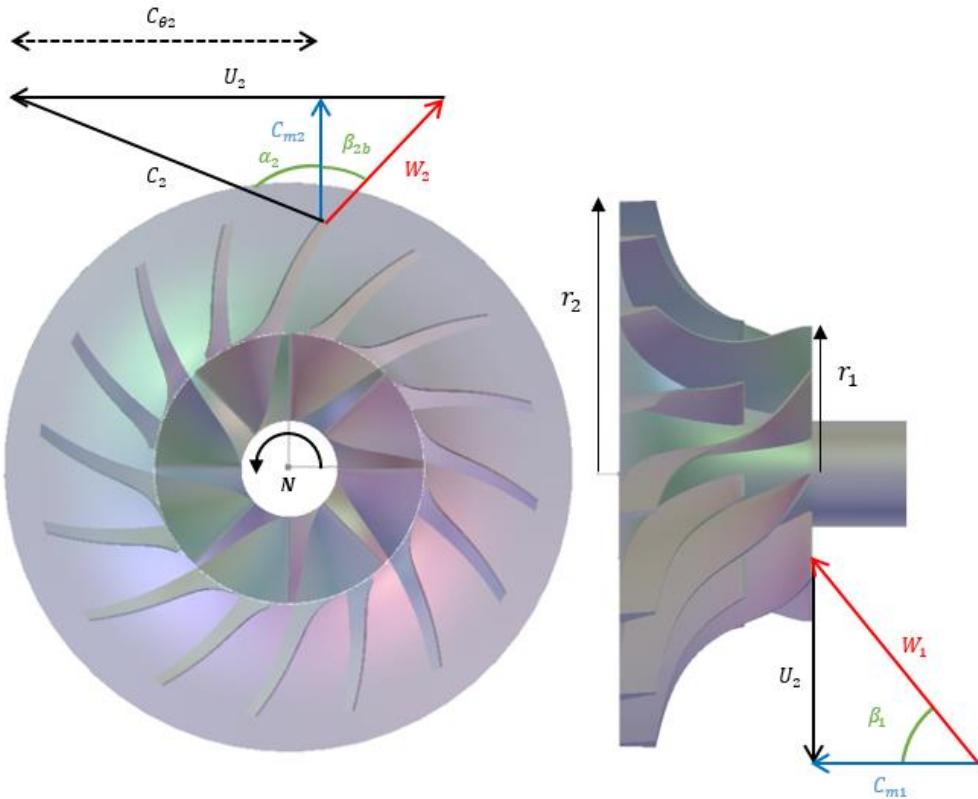
Figure 6: Typical velocity diagram for a centrifugal compressor

By applying conservation of momentum over the system, the external torque, τ, required to move a unit mass of fluid through the impeller can be calculated using *Equation 10*. This equation is known as the Euler Turbomachine Equation. It is the most important equation in turbomachinery, as it forms the basis for almost all performance characteristics (Boyce, 2006).

$$\tau = r_2 C_{\theta 2} - r_1 C_{\theta 1} [10]$$

Note that $C_{\theta 1}$ is omitted from *Figure 6*. This is because the fluid enters axially for a simple compressor inlet, and thus $C_{\theta 1}$ is equal to zero. Multiplying the torque by the rotational speed of the impeller, ω and the mass flow rate, $\dot{m}$, gives the power required for continuous flow:

$$W_c = \dot{m}(U_2 C_{\theta 2} - U_1 C_{\theta 1}) \ [11]$$

Note that the blade velocity, U, appears due to the multiplication of rotational speed and radius. By substituting this expression for compressor work into *Equation 6* the pressure ratio can be expressed as a function of the impellers geometry. *Equation 12* forms a key expression in the design of centrifugal compressors. It is important to note that this expression is simplified to ignore disk friction, cavity leakage, and recirculation work which are addressed later in *Section 4.2* for the final design (Japikse, 1996).

$$Pr = \left(\frac{\eta_{isen}(U_2 C_{\theta 2} - U_1 C_{\theta 1})}{C_p T_1} + 1 \right)^{\frac{\gamma}{\gamma - 1}} \quad [12]$$

This section has given a review of the fundamental aerodynamic characteristics that underpin the design centrifugal compressors without considering the mechanical or structural elements. The following section investigates the performance of commercially available compressors and designs done for specific studies that share similar requirements to the application of interest to this thesis.

2.2 Available designs

High speed centrifugal compressors find applications in the automotive and aerospace industries (Schleer, 2006). For these applications, they are typically employed in a turbocharger arrangement, where a turbine uses the exhaust gas of a combustion engine to drive a compressor impeller. The compressor impeller provides pressurised air to the engine to increase its combustion efficiency. The turbine is shown inside the red housing and the compressor within the blue housing in *Figure 7*.
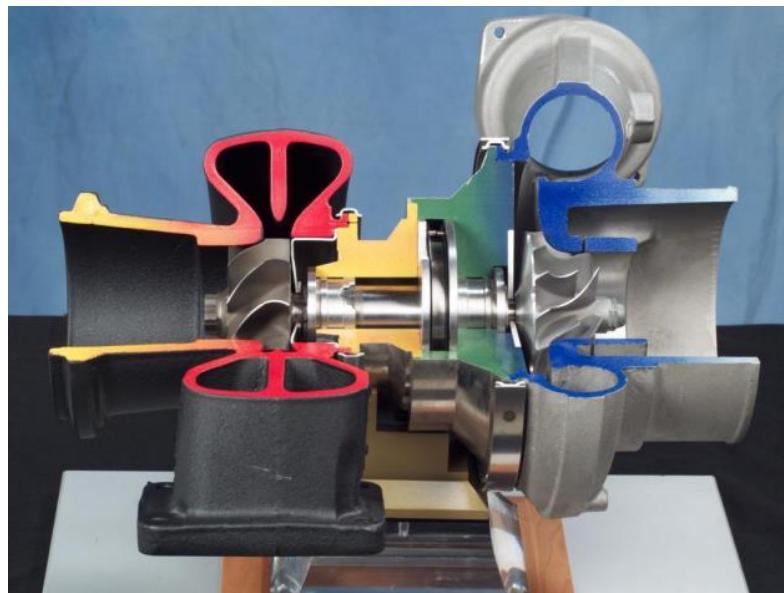
Figure 7: A typical turbocharger arrangement (Pope, 2009)

As discussed in *Section 1.4*, QGECE are currently developing a Holset HE351Ve model turbocharger for dissipation of 20kW of turbine power at 120kRPM. For the 100kW requirement, QGECE have found that there are no commercially available compressors that could be matched (Keep, 2016). *Figure 8* below shows a generalisation of the compressor maps superimposed on the same axes for the range of Holset turbochargers available. The curve shown in green on the figure highlights the 100kW line of constant power.
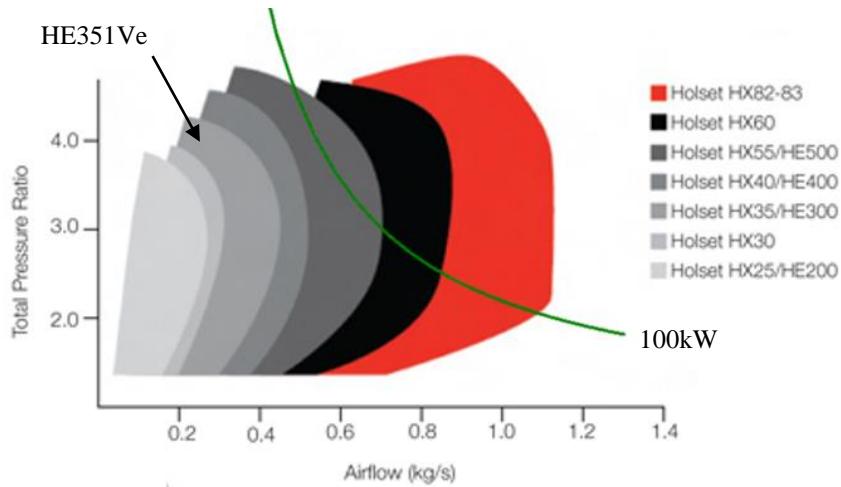
Figure 8: Range of Holset turbochargers (Holset, n.d.)

Figure 8 indicates that the speed requirement is the constraint on the compressor selection as opposed to power. The HE351Ve turbocharger which is highlighted on the figure is speed limited to ~130krpm. This limit is due to centrifugal stress. Impellers with larger diameters, manufactured by the same material must be limited to speeds lower then this to ensure they do not fail. Although models HX82-83, HX60 and HX55/HE500 provide a suitable pressure ratio and mass flow rate to dissipate 100kW of power, they do not meet the speed requirement of 120kRPM. Compressors made by different manufactures of similar sized compressors have similar performance as they are typically made from the same material (cast aluminium). It can therefore be concluded that the figure above is roughly representative of the market availability.

Numerous studies have been conducted into the design of high speed centrifugal compressors. J. Ling, K.C. Wong & S. Armfield (2007) at the University of Sydney wrote a paper on the development of a KKK2038 compressor wheel for a small gas turbine. Their final design, which was developed using CFD, showed a 71mm diameter backswept impeller rotating at 120kRPM. At the design point, the pressure ratio around 2.5 which only required 35kW of power (J.Ling, 2007).

H. Uchinda, M. Shiraki, A. Bessho & Y. Yagi (1994) described the method used to develop a centrifugal compressor for a 100kW automotive gas turbine. The design required a compressor that could provide a pressure ratio of 5 at 110kRPM. Using titanium alloy (Ti-6Al-4V), backswept impeller of 40° with 10 main blades and 10 splitter blades the compressor achieved a pressure ratio of 5 at 100kRPM (Hiroshi Uchida, 1994). B. Merwe (2012) also designed a centrifugal compressor impeller for a small gas turbine. The design was able to achieve a pressure ratio of 4.72 with a 75mm diameter impeller rotating at 121kRPM. Although no power requirement explicitly stated, back calculation from the compressor maps assuming ambient conditions gave approximately 30kW (Merwe, 2012).

A review of the literature and commercially available options indicates that designs have been completed around the rotational speeds, power requirements, impeller size and pressure ratio expected

for requirements of this design problem. None however, have been found to meet the combination of these requirements that are necessary for the dissipation of 100kW of power at 120kRPM.

The following section investigates the third design option which is the effect of controlling the inlet pressure and temperature of the air. The aim of the investigation was to assess whether the inlet properties can be controlled in such a way that the HE351Ve compressor would be employed for the 100kW requirement.

3 DESIGN OPTIONS

The literature review concluded that there were no commercially available compressors that could meet the combination of design requirements. The same result was concluded from investigation of custom designed impellers in other studies. Custom designing a compressor suited to this application, or controlling the inlet properties of the working fluid (air) are two design options that have potential to meet the requirements. The latter is investigated in this section using the compressor map of the HE351ve. *Section 3.1* outlines the effect of increasing temperature and *Section 3.2* demonstrates the effect of increasing pressure.

3.1 Increasing temperature

Figure 9 below shows the effect of increasing the inlet temperature (at constant pressure) of the air prior to it entering the compressor. The blue line shows the 100kW running line at an ambient temperature of 25℃ (298K). As shown, as the temperature increases the requirement line moves further toward the compressor map.
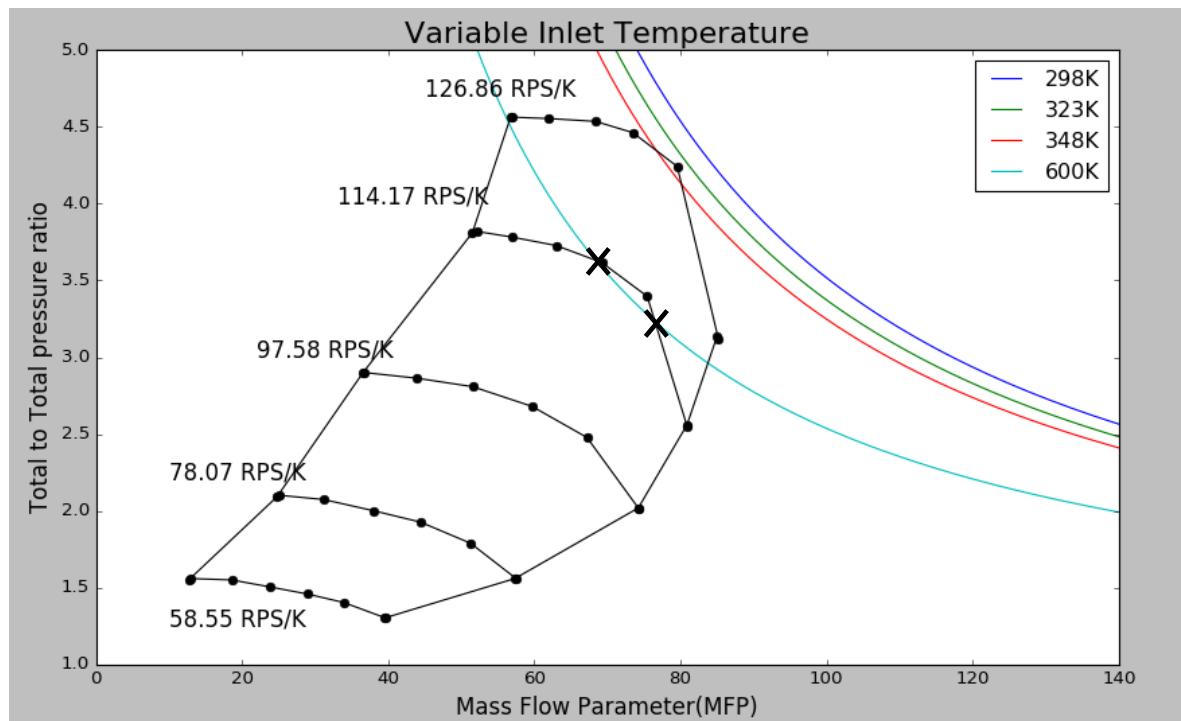
Figure 9: Effect of increasing inlet air temperature

The temperature of the inlet air required to shift the running line to a point that would meet the speed requirement is approximately 327℃ (600K) shown in light blue (recall that the speed requirement can be closely approximated by the 114.17rps/K speed curve). Note that this analysis does not take into account the reduction of density of the air when increasing the temperature at constant pressure. This change in density would cause the compressor map to rotate anticlockwise on this set of axis, as less mass would pass through the compressor for the same pressure ratio. The consequence of this is that heating the air to 600K without changing the pressure would still not provide the appropriate conditions

to match the 100kW requirement. Furthermore, higher temperatures can introduce creep of the aluminium impellers. This simple analysis demonstrates that increasing the temperature of the air is not a reasonable method to match the current compressor to the power requirement.

3.2 Increasing Pressure

Figure 10 shows the effect of increasing the inlet pressure (at constant temperature). The dark blue line shows the original 100kW line at ambient pressure of approximately 0.1MPa. As shown, relatively small increases in pressure result in large shifts of the line of constant power.
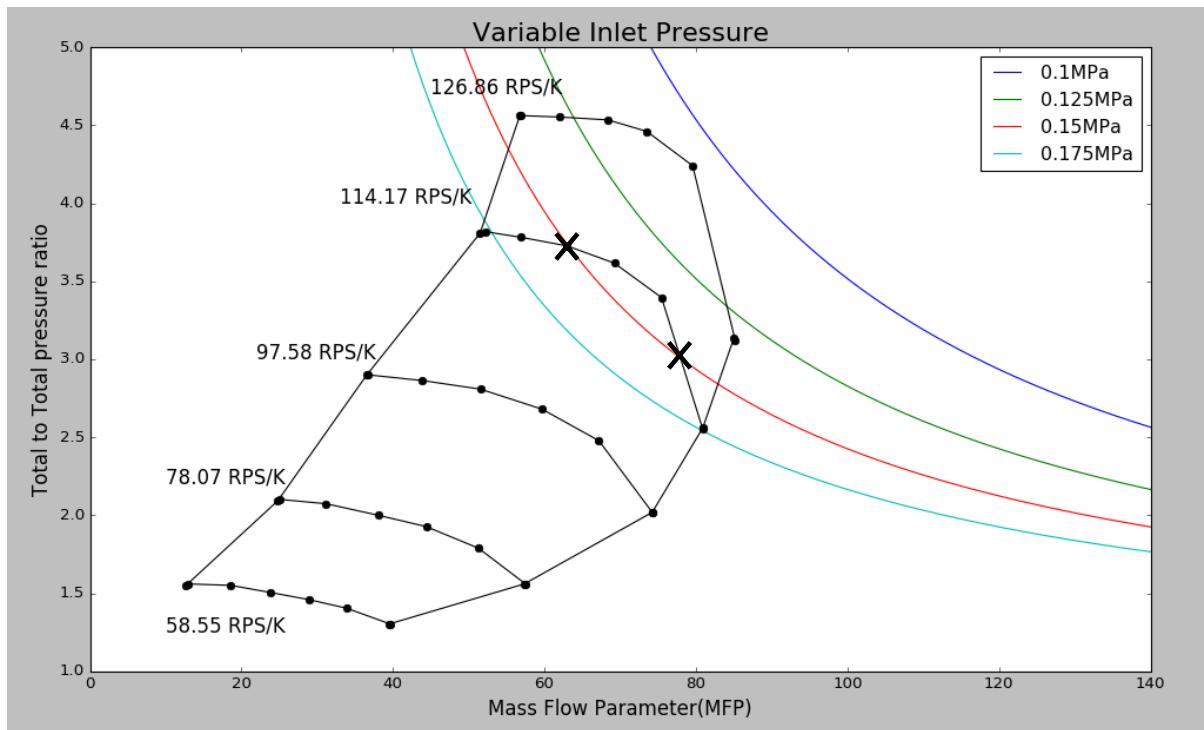
Figure 10: Effect of increasing air pressure

By increasing the pressure by 500kPa, the line of constant power is shifted to intersect with the appropriate speed curve. Again, this simplified analysis does not consider the change in density that would be brought about by pressurising the air. In practice, increasing the inlet pressure could be achieved through a recirculation system, where the compressor draws air from a pressurised vessel set to above 0.15MPa. The recirculation system would comprise of a pressure vessel, several valves to control the flow and a series of pipework to integrate the components. Additionally, an intercooler between the pressure vessel and compressor inlet may be required to control the increase in temperature brought about by pressurising the air in the vessel.

The literature review identified that using an alternative working fluid with a higher density and higher ratio of specific heats could lead to an effective solution. The purpose of this section however was to analyse whether controlling the inlet properties was a feasible design path to meet the requirements. The selection of working fluid would become part of a further study if designing a recirculation system

was pursued. The comparison between designing a recirculation system and designing a compressor to meet the requirements is outlined in the following section of this thesis.

3.3 Comparison and selection of design option

In order to select whether a recirculation system or custom compressor would be designed, the two options were compared by their relative cost, complexity and ability to meet the design requirements. The following points outline the comparison between each design path according to the three key criteria.

3.3.1 Cost estimate

Machining costs for turbine wheels were sourced previously by QGECE from a local manufacturer in Brisbane. The cost range was found to be within $5,000-$8,500 for a stainless steel turbine of 100mm diameter. The assumption that turbine wheel machining would be approximately the same as compressor impeller costs was made. Additionally, it was assumed that the size of the impeller required would be approximately 100mm as well. A diffuser and housing of the impeller could be taken from an off-the-shelf turbocharger of similar dimensions and would likely cost $500-$1,000 considering modifications may be necessary. An initial estimate was therefore, $5000-$10,000. The assembly and installation of the compressor at the test facility could be done internally by QGECE. A recirculation system would likely comprise of a pressure vessel, associated piping and several valves. An intercooler to control temperature could potentially be required. A pressure vessel with a volume capacity that is adequate to handle a large flow rate (estimated~ 0.5kg/s) would need to be approximately 1000L (0.5kg/s corresponds to ~400L/s). The vessel's working pressure limit would need to be 200-300kPa to ensure adequate pressure delivering to the compressor inlet. A stainless steel pressure vessel of this description would cost $12,000 (according to cost estimates published by Hanson Tanks online). The associated pipework and valve cost would be insignificant in comparison to the vessel. If an intercooler was necessary, this could elevate the cost significantly. Installation of the recirculation system could potentially require outsourcing.

3.3.2 Complexity

The design of compressors using simple 1-Dimensional equations is covered well in literature. The simple 1-Dimensional equations can calculate the geometry required for a particular application quickly and to within a useable accuracy. Designing a recirculation system however, would require consideration of multiple components and various Australian Standards (AS1210-2010 *Pressure Vessels*, AS4041-2016- *Pressure Piping* and AS1271-2003 *Safety Valves*). Additionally, the estimated volume and pressure capacity correspond to a B level hazard according to AS4334:2005 *Pressure Equipment-Hazard Levels*. This level of hazard would require registration and design verification with State Work Health and Safety Authorities which would likely add procurement difficulty and incur additional cost (FEC, 2013). Furthermore, QGECE staff supervising the study have extensive knowledge in the design of turbomachinery that could be leveraged.

3.3.3 Performance

The feasibility of both design options was established in the literature review. Commercially available compressors could deliver the required mass flow and pressure ratio, however, they were limited by speed which could be addressed by using a material that is stronger than cast aluminium. The preliminary assessment of the recirculation system showed that increasing the pressure moderately above atmospheric could achieve the design requirements using a commercial compressor.

Both systems were predicted to be able to meet the design requirements. The elevated cost and complexity of the recirculation system meant that designing a centrifugal compressor was selected. The remainder of this thesis focuses on the design of a centrifugal compressor. The following section presents the methodology used to develop the final design.

4 DESIGN METHODOLOGY

A 1-Dimensional mean line analysis was adopted in this study to establish the geometry and performance of the proposed centrifugal compressor. To establish the geometry, a Python script shown in *Appendix 8.3* was created based on the mean line analysis outlined by Japikse (1996). This analysis is detailed in *Section 4.1* and *Section 4.2*.

In a 1-Dimensional mean line analysis, the design of a centrifugal compressor is conducted for one mass flow rate and pressure ratio. Further to this nominal design, the off-design performance of a centrifugal compressor is quantified at anticipated points of operation. To do these calculations, NASA's FORTRAN model for predicting the off-design performance of centrifugal compressors was adapted into a Python script which is shown in *Appendix 8.4* (Galvas, 1973). The preliminary aerodynamic design procedure used in this study is summarised in *Figure 11* below. Each box represents a stage in the overall design process. The description in each box summarises the methodology used in each stage.

Established Geometry Code (5.1) Adapted the set of 1-D design equations from Japikse (1996) into a Python script	**Established Performance Code (5.2)** Adapted NASA's FORTRAN model for predicting the off-design performance of centrifugal compressors into a Python script
Established Geometry (6.1) Developed the geometry required to meet the design requirements	**Validated Both Codes (Appendix 8.1)** Validated the design and performance code with the known geometry and performance of an off-the-shelf centrifugal compressor
Established Performance (6.2) Developed a compressor map for the established geometry	**Matched Design with Application (6.2)** Matched the performance of the proposed centrifugal compressor with the design requirement
Proposed Design (6) Proposed the aerodynamic design for mechanical consideration	**Iterated design** Does the performance match the application?

Figure 11: Overall aerodynamic design procedure

4.1 Geometry Code

The design of the centrifugal compressor is broken into three key components. The inducer, impeller and diffuser. A schematic of the code used to design the inducer is shown in *Figure 12* below. The numbered subscripts correspond to the stage in the meridional path of the flow shown in *Figure 5* of the literature review. The values assigned to each input variable of the code are discussed in *Section 4.4.3* for the final design. The Python script for the geometry code is shown in *Appendix 8.3*.

Inputs:
Thermodynamic: $P_{00}, T_{00}, \dot{m}$
Designer's choice: N, α_1, r_{1h}
Empirical: β_1
Starting estimate: C_{m1}

Calculation:
$$C_{\theta 1} = C_{m1} tan(\alpha_1)$$
$$C_1 = \left(C_{m1}^2 + C_{\theta 1}^2 \right)^{1/2}$$
$$T_1 = T_{00} - C_1^2/2Cp$$
$$M_1 = C_1/\sqrt{\gamma R T_1}$$
$$P_1 = P_{00}(T_1/T_{00})^{\gamma/(\gamma-1)}$$
$$\rho_1 = P_1/R T_1$$
$$A_1 = \dot{m}/[\rho_1 C_{m1}(1 - B_1]$$
$$r_{t1} = (A_1/\pi + r_{1h}^2)^{1/2}$$
$$U_{1t} = 2\pi r_{t1} N/60$$
$$W_{1t} = \left[C_{m1}^2 + (U_{1t}^2 - C_{\theta 1}^2 \right]^{1/2}$$
$$\beta_1 = tan^{-1}[(U_1 - C_{\theta 1})/C_{m1}]$$

Iterate C_{m1} for minimum W_{1t}
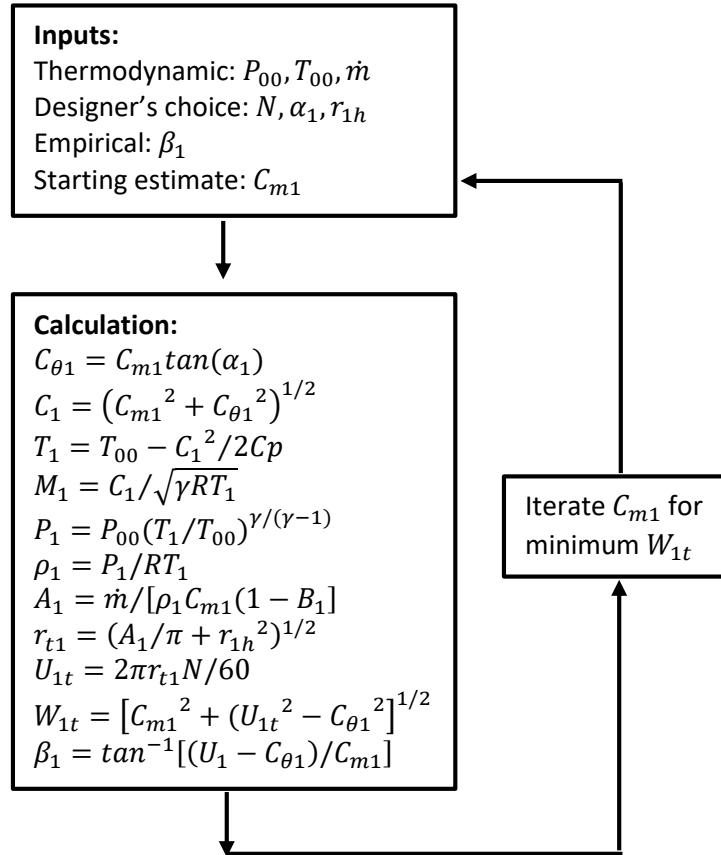
Figure 12: Design loop used to design the inducer (Japikse, 1996)

The schematic of the code used to design the impeller and diffuser is shown in *Figure 13*. Several additional inputs were required for the impeller and diffuser calculations. These are also outlined in *Section 4.4.3*. The impeller and diffuser design had two stages of iteration: one for the geometric parameters that calculate the slip factor and another that iterates the guessed efficiency until the output pressure ratio converges to desired the pressure ratio.

Inputs:
Thermodynamic: $P_{00}, T_{00}, \dot{m}, Pri$
Empirical: η, CpD
Designer's choice: $N, \lambda_{2m}, \beta_{2b}, Z_b, \eta_D, AR$
Starting estimate: η

Iterate:
Alter β_{2b}
and/or Z_b
and/or λ_{2m}

Impeller Calculation:
$\Delta h_{0s} = \gamma R T_{00}/(\gamma - 1)\ \left(Pr^{(\gamma-1)/\gamma} - 1\right)$
$W_x = \Delta h_0 = \Delta h_{0s}/\eta$
$T_{02m} = T_{00} + \Delta h_0\ (\gamma - 1)/\gamma R$
$\sigma = 1 - \sqrt{\cos(\beta_{2b})}/Z_b{}^{0.7}$
$\mu = \sigma \lambda_{2m}/(\lambda_{2m} - \tan(\beta_{2b}))$
$U_2 = [(U_1 C_{\theta 1} + W_x)/\mu]^{1/2}$
$D_2 = 60 U_2/\pi N$
$C_{\theta 2m} = \mu U_2$
$C_{m2m} = C_{\theta 2m}/\lambda_{2m}$
$T_{2m} = T_{02m} - (\gamma - 1)/2\gamma R\ \left(C_{\theta 2m}{}^2 + C_{m2m}{}^2\right)$
$P_{02m} = P_{00}[W_x \eta (\gamma - 1)/\gamma R\ T_{00}\ + 1]^{\gamma/(\gamma-1)}$
$P_{2m} = P_{02m}/(T_{02m}/T_{2m})^{\gamma/(\gamma-1)}$
$\rho_{2m} = p_{2m}/R\ T_{2m}$
$A_{2m} = \dot{m}/\rho_{2m} C_{m2m}$
$b_2 = A_{2m}/\pi D_2$
$C_2 = \left(C_{\theta 2m}{}^2 + C_{m2m}{}^2\right)^{1/2}$

Iterate:
Iterate η until
$Pr = Pri$

Check:
$$\frac{r_{1t}}{0.5 D_2} < e^{-8.16 \cos(\beta_{2b})/Z_b}$$

No

Yes

Diffuser Calculation:
$CpD_i = 1 - 1/AR^2$
$CpD = \eta_D CpD_i$
$P_3 = P_{2m} + CpD(P_{02m} - P_{2m})$
$C_3 = C_2/AR$
$P_{03} = P_3 + 1/2\rho_{2m} C_3{}^2$

Calculation:
$$\eta = \frac{(P_{03}/P_{00})^{(\gamma-1)/\gamma} - 1}{(T_{02m}/T_{00}) - 1}$$

$$Pr = P_3/P_{00}$$

Figure 13: Design loop used to design the impeller and diffuser adapted from Japikse (1996)

4.2 Off-Design Code

The code used to determine the off-design performance was adapted from NASA's FORTRAN model for predicting the off design performance of centrifugal compressors (Galvas, 1973). The code uses the output from the geometry code and establishes the off design performance by calculating a series of individual enthalpy losses that result from operating the compressor at off-design mass flow rates. These individual enthalpy losses are summed and used to calculate the overall efficiency for a particular mass flow rate. Each of these individual enthalpy losses are presented below as they appear in NASA's model. The variables that contribute to each loss are described. The calculation of each variable that contributes to the overall loss is not described here. These calculations can be found in the Python script shown in *Appendix 8.4*. The code adapted for this study differs from NASA's model in three ways:

1. Losses from inlet guide vanes were not considered

2. Losses from the vaned diffuser were not considered

3. A constant static pressure recovery coefficient in the vaneless diffuser was assumed rather than modelling how it varies at different mass flow rates.

Losses from the inlet guide vanes and vaned diffuser were not considered because neither of these components were considered in the final design, nor are they used in the compressor model the code was validated against. A constant static pressure recovery coefficient was chosen to simplify the calculation and because it was assumed that it would not change dramatically over the operating range of the diffuser.

Inducer incidence loss: losses due to the change in incidence angle at the inducer.

$$\Delta h_{INC} = \frac{W_L{}^2}{2Cp} [13]$$

Where, W_L is the component of relative velocity lost due to the change in incidence angle at the inducer.

Blade loading loss: losses caused by the aerodynamic loading of the impeller blades (Galvas, 1973).

$$\Delta h_{BL} = 0.05 D_f{}^2 U_2{}^2 [14]$$

Where, D_f is the diffusion factor and U_2 is the exit blade tip speed.

Skin friction loss: losses due to friction of the blade and hub surfaces of the impeller.

$$\Delta h_{SF} = K_{DF} C_f \frac{\frac{L}{D_2}}{\frac{D_{HYD}}{D_2}} \left(\frac{W}{U_2}\right) U_2{}^2 [15]$$

Where K_{DF} is 7.0 for impellers with splitter blades and 5.6 for impellers without splitter blades, C_f is the friction coefficient, $\frac{L}{D_2}$ is the length to diameter ratio, $\frac{D_{HYD}}{D_2}$ is the ratio of the hydraulic diameter to the exit diameter and $\frac{W}{U_2}$ is the ratio of relative velocity to exit blade speed.

Disk friction loss: losses due to windage on the compressor back face.

$$\Delta h_{DF} = 0.01356 \frac{\rho_2}{\dot{m} Re^{0.2}} U_2{}^3 D_2{}^2 [16]$$

Where, ρ_2 is the density at the outlet of the impeller, Re is the Reynolds number, D_2 is the diameter at the exit and $\dot{m}$ is the mass flow rate.

Recirculation loss: losses resulting from work done on the working fluid due to backflow into the impeller (Galvas, 1973).

$$\Delta h_{RC} = 0.02 \sqrt{\tan(\alpha_2)} D_f{}^2 U_2{}^2 [17]$$

Where, α_2 is the absolute angle of the exiting flow.

Vaneless diffuser loss: losses as the flow passes through the vanless space.

$$\Delta h_{VLD} = Cp T_2' \left[\left(\frac{P_3}{P_3'} \right)^{(k-1)/k} - \left(\frac{P_3}{P_2'} \right)^{(k-1)/k} \right] [18]$$

Where, Cp is the specific heat at constant pressure, T_2' is the relative temperature at the impeller exit, $\frac{P_4}{P_4'}$ is the ratio of absolute to relative pressure at the diffuser exit and $\frac{P_4}{P_3'}$ is the ratio of the absolute pressure at the diffuser exit to the relative pressure at the impeller exit.

The combination of enthalpy losses is then used to establish the overall efficiency of the compressor which is shown in *Equation 19*:

$$\eta = \frac{\Delta h_{aero} - (\Delta h_{INC} + \Delta h_{BL} + \Delta h_{SF} + \Delta h_{VLD})}{\Delta h_{aero} + \Delta h_{RC} + \Delta h_{DF}} [19]$$

Where Δh_{aero} is the enthalpy rise throughout the impeller.

Both the geometry and off-design codes were validated against a commercially manufactured compressor. The compressor selected for the validation was the GT1548 turbocharger compressor manufactured by Garrett. This compressor was chosen as its geometry and performance are published online and are easy to access. The full validation procedure is outline in *Appendix 8.1*. From the validation process the following limitations to the accuracy of the geometry and off-design codes were identified:

- Both the geometry and performance codes are sensitive to the empirical values that are used. The empirical values include the friction coefficient, blockage factor and swirl parameter which are chosen based on literature and best estimates which limits the robustness of the code.

- The off design performance code does not take into account shock losses.

- The model assumes that the static pressure recovery in the diffuser is constant for all operating points. This does not occur in real compressors.

- The equations used to calculate slip are based on geometric parameters only, however the slip may vary substantially for each speed contour (Japikse, 1996).

With the following limitations considered, both codes were deemed valid for use in the design of the centrifugal compressor to meet QGECE's requirements.

4.3 Design Strategy

In *Section 2.2* it was noted that the commercially available compressors able to dissipate 100kW of power were limited by speed. The aluminium cast used for commercial impellers sets the centrifugal stress limit and consequently the maximum outlet tip speed for a given shaft speed. The strategy adopted to meet the design requirements was therefore to select a material that had a higher centrifugal stress limit. The impeller would then be designed to have a maximum outlet diameter and minimum inlet diameter. Maximising the diameter would increase the envelope of mass flows over which the compressor would dissipate 100kW. This is important as the compressor is designed based on one mass flow rate, which may not be the mass flow rate it operates at when installed. Minimising the inlet increases pressure ratio. The increased pressure ratio results in a lower mass flow rate required to dissipate the power. When designing to avoid choke, a lower mass flow rate is desirable.

The geometry and off-design models are suitable for the preliminary design of a compressor where high off-design efficiency is essential. It is important to note that the commercially manufactured compressors are designed for high off-design efficiency and long-term reliability. These requirements were not criteria of the current design. High efficiency is not of concern because the power is being dissipated rather then delivered. In addition, the application of the compressor is for a test facility where experiment time is short relative to the typical operating time of turbochargers. Consequently, the reliability of the compressor did not need to be long-term. This meant that the compressor could be operated closer to its maximum stress limits.

The mass flow rate and pressure ratio required to dissipate 100kW of power are established in the following two sections. Note that these calculations were not part of the geometry or off-design codes. Instead, the calculations were completed by hand and used as the inputs to the geometry code. The strategy to meet the requirements was to design the compressor to operate at a slightly higher mass flow and pressure ratio than is required to dissipate the power. This would mean that the design point would

lie above the 100kW line of constant power. The off design envelope would intersect the line of constant power at two points if designed correctly, providing two operating points of which 100kW of power would be dissipated at 120kRPM.

4.4.1 Speed Requirement

Centrifugal stress is the limitation of higher blade tip speeds for the commercially available compressors previously investigated. By modelling the impeller as a solid disk the centrifugal stress at the exducer radius can be calculated using *Equation 20*:

$$\sigma' = \frac{3+v}{8}\rho\omega^2 r_2{}^2 \,[20]$$

The corresponding displacement at the exducer radius is:

$$u = \frac{1-v}{4E}\rho\omega^2 r_2{}^3 \,[21]$$

Where v, in both equations is Poisson's ratio and E is Young's modulus. By inspection of *Equation 21* it is clear that materials with a high Poisson's ratio, high Young's modulus and low density are desirable for high speed applications. A maximum speed limit for a given material and outlet radius can be calculated by rearranging *Equation 20* for ωr_2, which represents the absolute blade tip speed in meters per second:

$$\omega r_2 = \sqrt{\frac{8\sigma_y'}{(3+v)\rho}} \,[22]$$

Where σ_y' is the yield strength of the material. *Table 5* summarises this calculation for materials commonly used to design turbomachinery. The data for each material was taken from Aerospace Specification Metals Inc.

Table 5: Speed limitations of typical materials used in turbomachinery design

Material	Designation	Density (kg/m³)	Poisson's Ratio	Yield Strength (MPa)	Speed limit (m/s)
Cast aluminium	AL C355 T-6	2800	0.33	200	414
Machined aluminium alloy	AL 2618 T-61	2700	0.33	370	574
Machined titanium alloy	Ti 62460	4430	0.342	950	716
Machined titanium alloy	Ti 6242	4540	0.32	990	724

Machined titanium impellers are able to tolerate much higher speeds than aluminium impellers based on this simplified disk stress analysis and hence only these materials were considered further for selection. In order to distinguish between the two titanium grades, the machinability was considered.

An assumption was made that the alloy with the higher machinability would result in a lower overall cost for the impeller. An equation to calculate the machinability was taken from Juvinall. R (2011). *Equation 23* describes the cutting speed, V_{60}, in ft/min for 60-minute tool life under standard cutting conditions (Juvinall. R, 2011):

$$V_{60} = \frac{1150k}{H_B}(1 - A_r)^{1/2} [23]$$

Where k is the thermal conductivity in Btu/(h ft °F), H_B is the Brinell hardness number and A_r is the area reduction at fracture. *Table 6* summarises the machinability comparison of Ti 62460 and Ti 6242.

Table 6: Comparison of machinability between titanium alloys

Material designation	Thermal conductivity (Btu/(h ft °F)	Birnell hardness number	Area reduction at fracture (%)	Cutting speed (V_{60})
Ti 62460	46.5	334	36	128
Ti 6242	49.3	318	25	154

Given the machinability of Ti 6242 is higher than Ti 62460, and their respective maximum speeds are the same, Ti 6242 was selected for the impeller design. Japikse (1996) states that moderate life machined titanium alloys are able to tolerate speeds up to 670m/s. Given that the physical and mechanical properties of alloys can fluctuate depending on where they are sourced, and to take a conservative approach in the design, 670m/s was selected as the speed limit for the titanium. This allowed for the calculation of the maximum diameter based on the speed requirement, N of 120kRPM and the maximum exit blade speed U_2, 670m/s:

$$D_2 = \frac{N/60}{2\pi U_2} [24]$$

$$D_2 = 106.6mm$$

105mm was selected as the exit diameter of the impeller in order to operate slightly below the maximum speed. This diameter corresponds to an exit speed of 660m/s. This dimension became the constraint to calculate the mass flow rate and the pressure ratio required to dissipate 100kW at 120kRPM.

4.4.2 Power Requirement

To meet the power requirement, the pressure ratio and mass flow rate needed to be established as inputs for the design code. From the Euler turbomachinery equation, the work done by the compressor can be calculated by:

$$W_c = \dot{m}(U_2 C_{\theta 2} - U_1 C_{\theta 1}) [25]$$

For an axial inlet duct where the entering air is not subject to pre-swirl, the tangential component is zero ($C_{\theta 1} = 0$). *Equation 25* becomes:

$$W_c = \dot{m}(U_2 C_{\theta 2}) [26]$$

Where,

$$C_{\theta 2} = \mu U_2 [27]$$

Where μ is the work input coefficient, which is calculated from; the impeller back sweep angle, β_{2b}, number of blades, Z_b and the swirl parameter, λ_{2m}. μ was calculated to be 0.616.

Hence, the design mass flow rate was:

$$\dot{m} = \frac{W}{\mu U_2^{\ 2}} [28]$$

Using the power requirement, work input coefficient and the maximum tip speed, the mass flow rate required was:

$$\dot{m} = \frac{100000}{0.616 \times 660^2} = 0.373 kg/s$$

The required pressure ratio was calculated using a re-arrangement of *Equation 6* established in *Section 1.4*:

$$Pr = \left[\frac{\eta_{isen} W_c}{C_p T_1} + 1 \right]^{\frac{\gamma}{\gamma - 1}} = \left[\frac{\eta_{isen} \mu U_2^{\ 2}}{C_p T_1} + 1 \right]^{\frac{\gamma}{\gamma - 1}} [29]$$

Where, w_c is the work per unit mass. The efficiency, η_{isen} was approximated to be 0.6. This value is justified in the *Section 4.4.3*.

Using the required values and the assumption of a standard air temperature, the pressure ratio required was:

$$Pr = \left[\frac{0.6 \times 0.616 \times 660^2}{1005 \times 293} + 1 \right]^{\frac{1.4}{1.4 - 1}} = 4.6$$

In order to design the compressor for a point that would lie above the 100kW line, a mass flow rate of 0.4kg/s and pressure ratio of 4.8 were selected for the design. These two inputs formed the basis of the design and performance code. Other inputs important to the code are outlined in the following section.

4.4.3 Code Inputs

Table 7 shows the value assigned to the variables that serve as inputs to the design and performance codes. The variable, its corresponding value and a justification is provided.

Table 7: Justification of variable inputs for geometry and off-design code

Variable	Value	Justification
Hub radius, r_{1h}	$10mm$	The turbine output shaft that the compressor impeller will be coupled to has a radius of 8mm. A slightly higher hub radius was needed to facilitate the connection of the shaft and compressor impeller.
Boundary layer blockage, B_1	0.04	The boundary layer blockage depends on the shape of the inlet duct. Empirical values for various inlet shapes are given in Japikse (1996). The inlet duct was chosen to be a simple, axial inlet corresponding to 0.04 for the boundary layer blockage.
Exit swirl parameter, λ_{2m}	2	Lower values of lambda can attribute to improved range and rotor diffusion (Japikse, 1996). Additionally, lower lambda values contribute to lower work input coefficient and consequently lower mass flow rate to dissipate 100kW of power.
Impeller back sweep, β_{2b}	$-40°$	Higher back sweep can correspond to slightly higher efficiencies and improved range at higher pressure ratios when running at 100% speed (Japikse D. , 1996). Because the design is operating at both its design speed and higher pressure ratios, a high back sweep angle was selected. Additionally, as discussed in *Section 2.2*, H. Uchinda *et al* (1994) designed a 100kW machined titanium compressor impeller. Their design featured 40° back sweep. This verified the degree of back sweep chosen in this design.
Predicted efficiency, η	60%	Because the exducer speed was set to 660m/s, the exiting flow could potentially reach or exceed Mach 1, causing shock wave formation. Shock losses result in a reduction of efficiency. Thus it was expected that the peak compressor efficiency would operate at the lower range of commercially available compressors $\sim$60%.
Number of blades, Z_b	16	This included 8 full blades and 8 splitter blades. Splitter blades have been shown to improve performance for impellers with high back sweep (Japikse D. , 1996). The number of blades was selected by comparing the size of the impeller to those of commercial impellers. The GT4202R and the Holset HX80 which feature similar outlet

Variable	Value	Justification
		diameters have 8 splitter and 8 full blades. This was the basis for the decision to select 16.
Area ratio of the diffuser, AR	2.5	The area ratio of the diffuser is the area swept out by the edge of the vaneless diffuser divided by the area swept out by the exducer. This area is largely responsible for the static pressure rise throughout the compressor. 2.5 was chosen based on similar sized commercial compressors and because it allowed sufficient pressure recovery through the diffuser.
Diffuser efficiency η_d	85%	QGECE recommended a value of approximately 0.7 to be used for the static pressure recovery coefficient in the diffuser. 85% diffuser efficiency was found to correspond to a static pressure recovery coefficient of 0.714 for the estimated area ratio. The diffuser efficiency was assumed to remain unchanged for all operating points.
Blade thickness, t_u	$2mm$	Selected based on typical blade thickness for machined impellers.
Hub and tip curvature, $curvet1, curveh1$	0°	No curvature of the hub and blade is required for subsonic inducers (Japikse, 1996).
Streamline angle, x	10°	Selected to match typical commercial compressors.
Blading loss coefficient, kBL	0.6	The blading loss coefficient was 0.75 for impellers without splitters and 0.6 for impellers with splitters (Galvas, 1973).
Skin friction coefficient, kSF	7	Skin friction coefficient is designated as 5.6 for impellers without splitters and 7 for impellers with splitters. The coefficients account for the increase in average relative velocity resulting from the use of splitters. (Galvas, 1973)
Blade friction coefficient, C_f	0.01	Selected based on the mean friction coefficient versus radius ratio given by Japikse & Baines (1997).

5 PROPOSED DESIGN

5.1 Geometry

The final geometry of the compressor is summarised in *Table 8,* in addition to its performance at the design point. The design features a large exducer and a narrow inducer. These features are typical of a high pressure ratio, moderate mass flow rate compressor. The inducer is designed to be significantly smaller than off-the-shelf titanium impellers to increase the pressure ratio when operating at 120kRPM. A narrow inducer is the reason why an off-the-shelf titanium impeller could not be employed for this application. The trade-off between high pressure ratio and low efficiency as a result of narrowing the inlet, is not of interest to centrifugal compressor designers. At the design point, the proposed compressor is predicted to dissipate 110kW of power at 56% efficiency. *Section 5.2* demonstrates that the selected design point was sufficient to dissipate 100kW of power at other mass flow rates.

Table 8: Dimensions and performance at the design point

Feature	Dimension
Exducer diameter	105mm
Inducer tip diameter	55mm
Inducer hub diameter	20mm
Number of blades (splitters)	8 (8)
Blade thickness	2mm
Exit blade height	4.2mm
Work dissipation at design point	110.949kW
Rotational speed	120kRPM
Mass flow rate at design point	0.4kg/s
Pressure ratio at design point	4.4
Efficiency at design point	56%
Diffuser exit diameter	166mm

The iteration process to minimise the relative component of velocity at the inducer (W_{1t}) found the absolute component of velocity for the design (C_{m1}) to be190m/s. This subsonic inlet meant the inducer did not need to be re-designed for transonic or supersonic speeds. This would typically require an adjustment of the hub and tip curvature ($curvet1, curveh1$).

The overall impeller dimensions are shown in the meridional view in *Figure 14.* The horizontal blue dotted line shows the rotation axis of the impeller. The vertical blue dotted line shows the plane that is swept out by the impeller. The numbers 0, 1, 1a and 2 correspond to the stage calculation used in the code. These stages were outlined in *Section 2.1*.

$b_2 = 4.2mm$

2

Shroud side

Inlet duct

$r_2 = 52.5mm$

$r_{1t} = 27.5mm$

0   1   1a

Hub side

$r_{1h} = 10mm$

Rotation axis
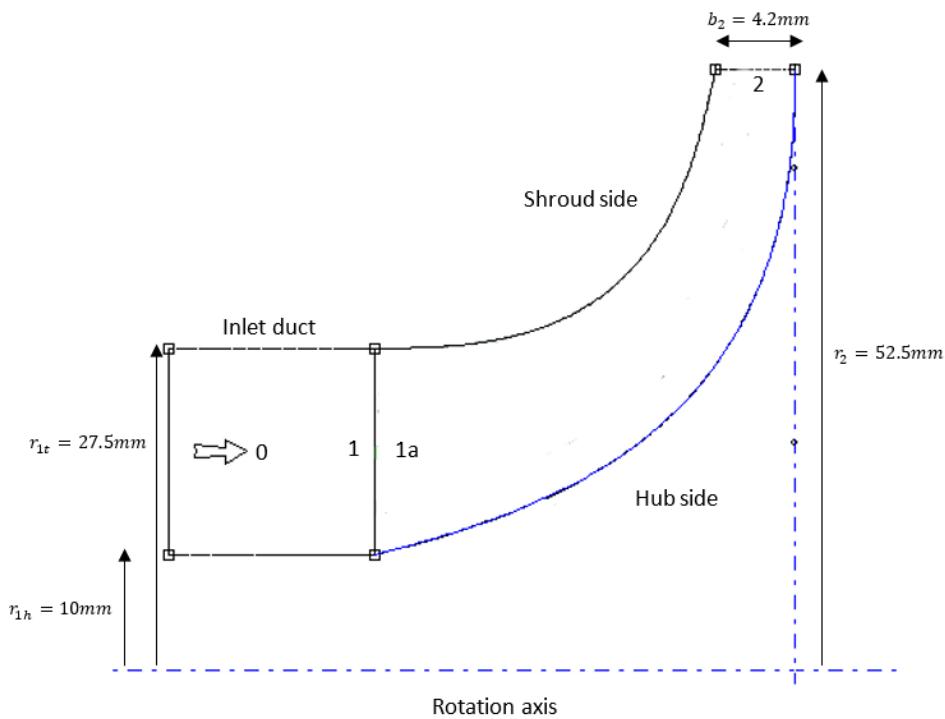
Figure 14: Meridional view of the impeller design

The geometry and performance of the designed impeller were uploaded into ANSYS BladeGen to visualise the final design. This is shown in *Figure 15.* A wireframe perspective of the final design is also shown in *Figure 16.* The green and black mesh show the hub and shroud of the impeller respectively. The red mesh shows the impeller blades and the pink highlights the interface between the blade edges and the shroud (housing).
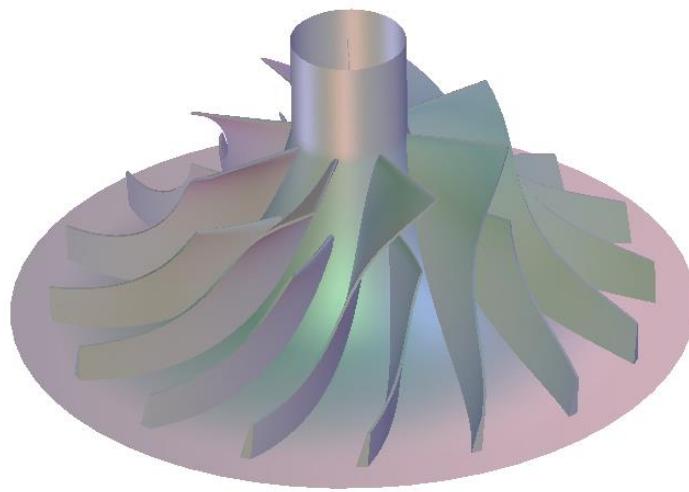
Figure 15: Final impeller design
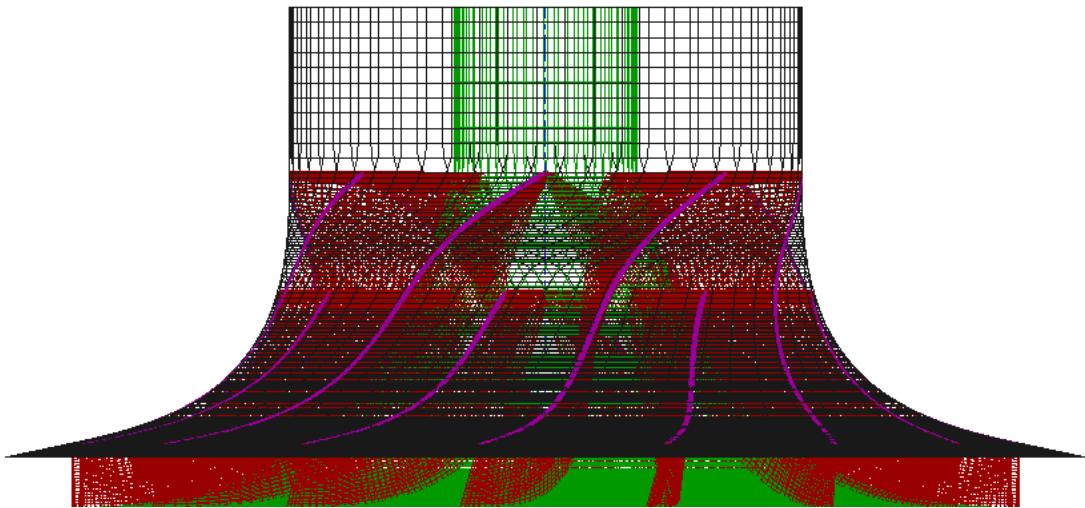
Figure 16: Wireframe perspective of the final impeller design

5.2 Performance

Figure 17 below shows the full 120kRPM operating envelope, superimposed over the 100kW line of constant power. The figure demonstrates that there are two points of intersection, each corresponding to operating points that can dissipate 100kW of power. These occur 0.292kg/s mass flow, 6.4 pressure ratio and 0.463kg/s mass flow, 3.6 pressure ratio. These two points demonstrate the design's ability to meet the requirements. The intersection at (0.292, 6.4) in *Figure* 17 would correspond to the physical operating point of the compressor, because it is located further from the choke region.
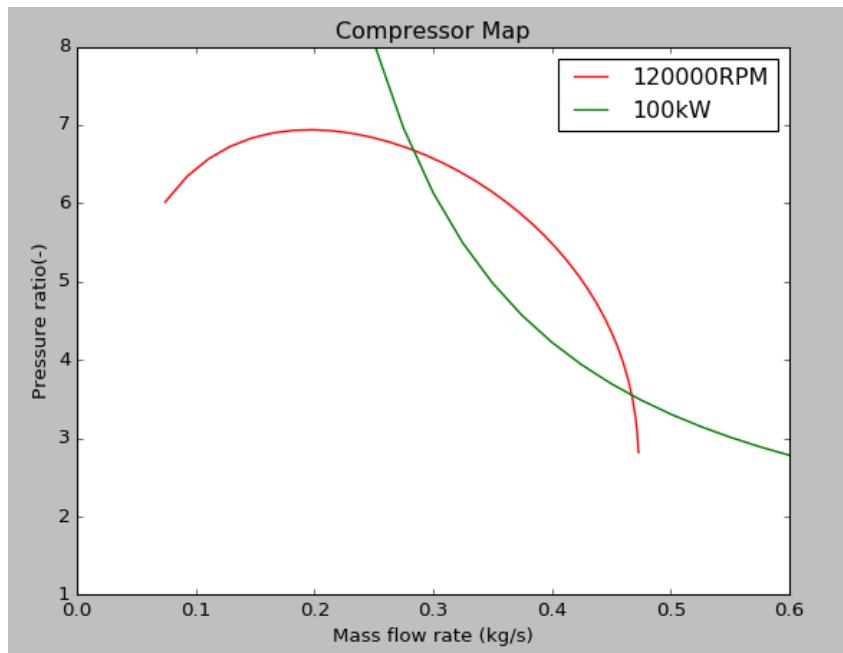
Figure 17: Performance envelope of the designed compressor at 120kRPM running speed

The efficiency contour is shown in *Figure 18*. The graph demonstrates efficiency increases with mass flow rate to a peak of 83.4% prior to choke. The same observation was made by Galvas (1973) in

comparing predicted performance against measured data of efficiency. The rapid drop in efficiency that occurs moving further into the choke region was not calculated due to an inability of the off-design code to calculate performance beyond this point.
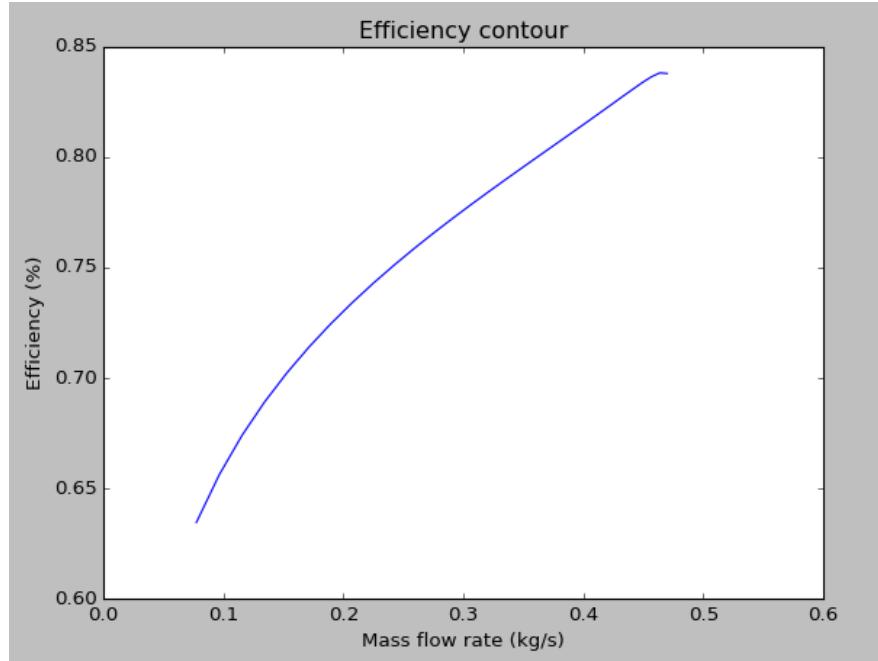
Figure 18: Efficiency contour of the designed compressor at 120kRPM running speed

The inlet velocity diagram is shown in *Figure 19* at the root-mean-square radius of the inducer; which is 21mm from the rotation axis. The diagram is shown with the velocities that correspond to the design mass flow rate of 0.4kg/s. Note that the velocity diagram does not show slip velocity at exit.
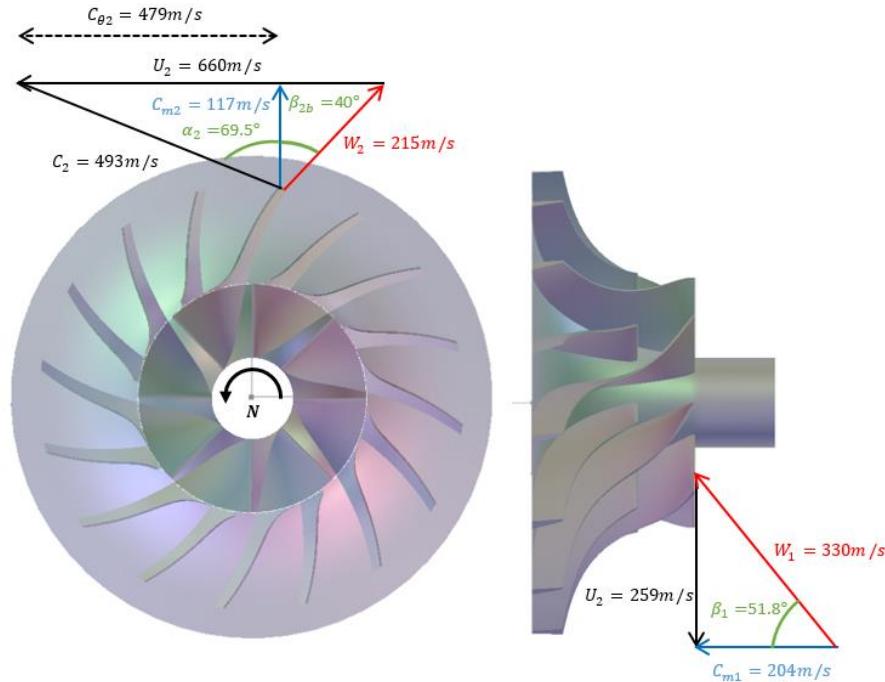
Figure 19: Velocity triangles for the inlet and outlet at the design mass flow rate.

The off-design code calculated that the velocity slightly exceeded Mach 1 at the impeller exit for some mass flow rates. This means that the impeller exiting flow will be between a transonic and supersonic state. Supersonic flow at the exit would result in the formation of shock waves which is not accounted for in the off-design code. This has three implications on the results of this analysis:

1. The pressure ratio is over predicted

2. The efficiency is over predicted

3. The work done by the impeller is under predicted

Physically, this would mean that the impeller would dissipate the 100kW of power at a lower pressure ratio and efficiency than predicted by the off-design code. The geometry code predicted the efficiency of the impeller at the design point to be 56%. It is likely that the efficiency would range between ~35-60% for the full operating range at 120kRPM. An adaption of the geometry and off-design codes would need to be performed to better characterise the efficiency and pressure ratio at which the design requirements are met.

An area ratio of 2.5 for the diffuser was required to achieve the specified performance. The inner diameter of the diffuser was equal to the exducer diameter of the impeller. A diffuser that fits this description is the diffuser from the GT4508R turbocharger manufactured by Garrett. The compressor impeller used for the GT4508R has a 108mm exducer and 80.8mm inducer. Hence, the inlet duct of the housing would need to be narrowed by approximately 25.8mm. This could be done in-house by QGECE, by fitting an internal sleeve to the inlet duct. A modified off-the-shelf housing coupled with the custom impeller was chosen based on the assumption that the housing design is not critical to power dissipation and that the cost to manufacture a new design would be expensive and unnecessarily time consuming to design.

5.3 Bill of Materials

The final dimensions are repeated in *Table 9* along with the operating points where the design requirements are met.

Table 9: Final dimensions and operating points that meet design requirements

Feature	Dimension
Exducer diameter	105mm
Inducer tip diameter	55mm
Inducer hub diameter	20mm
Number of blades (splitters)	8 (8)
Blade thickness	2mm
Exit blade height	4.2mm
Work dissipation	100kW
Rotational speed	120kRPM
Mass flow rate	0.292, 0.493
Pressure ratio	6.4, 3.6
Impeller material	Ti 6242
Diffuser exit diameter	166mm
Diffuser selection	GT4508R

Table 10 presents the Bill of Materials for the proposed design. The machined titanium impeller cost was based on a quote from Naeco; a local company proficient in Computer Numerically Controlled (CNC) machining. The housing of the GT4508R compressor is included along with a cost estimate for the required modifications. The housing cost shown is for the full purchase price of the turbocharger. This was based on the assumption that compressor housings are not sold individually. The cost estimate for the modification is based on published prices by Turbo Lab for Garrett housing modifications.

Table 10: Bill of Materials for the proposed design

Component	Specification	Sourcing strategy	Estimated Cost
Impeller	Machined titanium alloy Ti 6242	Machined by Naeco	$7000-$10,000
GT4508R Housing	GT4508R from Garret	Purchase from Garrett	$2000-$3000
Housing modifications	GT4508R from Garret	Modifications done by QGECE	$200

6 CONCLUSIONS AND FINAL RECOMMENDATION

The Queensland Geothermal Energy Centre of Excellence (QGECE) require a device that could dissipate 100kW of turbine power with a shaft rotational speed of 120kRPM. The device is to be installed at QGECE's power cycle test facility in Pinjarra Hills, Brisbane. This study has presented the design of a centrifugal compressor that meets these requirements.

A recirculation system was considered as an alternative approach to meet the design requirements. Estimated cost, complexity of design and performance were used as criteria to assess the feasibility the design options. The lower estimated cost and simplicity of the impeller design meant that it was chosen over the alternative for further development.

The geometry and off-design performance of the compressor were calculated using 1-Dimensional mean line analysis tools that were adapted into two Python scripts. The model for the geometry calculations was adapted from Japikse (1996). The off-design performance code was adapted from NASA's FORTRAN model for predicting the off design performance of centrifugal compressors (Galvas, 1973). Both codes were validated against a commercially manufactured centrifugal compressor (model GT1548 manufactured by Garrett).

The proposed design features a 105mm diameter machined titanium alloy impeller coupled with a modified GT4508R off-the-shelf housing. The compressor was shown to dissipate 100kW of power at two operating mass flows; 0.292kg/s and 0.463kg/s. These mass flows correspond to pressure ratios of 6.4 and 4.6 respectively. The overall cost estimate was found to be $9,200-$13,200.

Due to the high rotational speed and large exducer diameter, the exiting flow was found to slightly exceed Mach 1. The accuracy of the off-design code was limited to subsonic flow and thus the proposed performance of the design was over predicted. Future work on this design should include provision for shock losses in the off-design code. Additionally, the off-design code should be developed to account for changing static pressure recovery through the diffuser.

The performance envelope of the final design demonstrated that it was able to meet the requirements of 100kW of power at 120kRPM. The following recommendations address further work on this topic:

- The inducer diameter and impeller back sweep could be increased to reduce the Mach number at the exducer to less than 1. This would avoid shock formation at the impeller exit and allow the 1-Dimensional off-design code to accurately predict the compressor pressure ratio and efficiency. Changing these parameters would require the consideration of a trade-off between the larger mass flow and lower pressure ratio that would result.

- A CFD analysis should be performed on the final geometry to increase the confidence of the designs ability to meet the requirements. A CFD analysis would allow for a better

characterisation of the flow at each stage throughout the compressor and hence provide a more rigorous confirmation of the design.

- An analysis of the aerodynamic thrust caused by the impeller should be considered to the assess the loading on housing bearings and turbine shaft.

The load dissipation device presented in this thesis in the form of a centrifugal compressor will allow QGECE to conduct tests on supercritical turbines of power output up to 100kW. These tests allow QGECE to demonstrate their capability in designing supercritical CO_2 turbines which have application in renewable power generation.

7 REFERENCES

Boyce, M. P. (2006). Principles of operation and performance estimation of centrifugal compressors. *Proceedings of the Twenty-Second Turbomachinery Symposium*, 161-177.

FEC. (2013, May 10). Retrieved from Pressure Vessel Registration Requirements - Australia: https://www.feconsult.com/news/49-pressure-vessel-registration-australia

Galvas, M. (1973). *Fortran program for predicting the off-design performance of centrifugal compressors.* Cleveland, Ohio: Lewis Research Centre & U.S army air mobility R&D Laboratory.

Hiroshi Uchida, M. S. (1994). Development of Centrifugl Compressor for 100kW Automotive Ceramic Gas Turbine. *Internation Gas Turbine and Aeroengine Congress and Exposition.* The Hague, Netherlands: ASME.

Holset. (n.d.). *Holset Turbos, Model Information*. Retrieved from myholsetturbo: http://www.myholsetturbo.com/modelinfo.html

J.Ling, K. W. (2007). Numerical Investigation of a Small Gas Turbine Compressor. *16th Australasian Fluid Mechanics Conference* (pp. 961-966). Gold Coast, Australia: School of Aerospace, Mechanical & Mechatronic Engineering, University of Sydney.

Japikse. (1994). *Introduction into Turbomachinery.* United States of America: Concepts ETI, Inc. and Oxford University Press.

Japikse&Baines. (1997). *Diffuser Design Technology.* White River Junction: Edwards Brothers Inc.

Japikse, D. (1996). *Centrifugal Compressor Design and Performance.* Widler, Vermont: Thomson-Shore.

Juvinall. R, M. (2011). *Fundamentals of Machine Component Design.* Hoboken: John Wiley & Sons.

Keep, J. (2016). *Design scope for load dissipation compressor for supercritical CO2 turbines, Design Report.* Brisbane: QGECE.

Manjunath DC, R. D. (2014). Performance Investigation of High Pressure Ratio Centrifugal Compressor using CFD. *Internation Journal of Ignited Minds*, 1-6.

Merwe, B. B. (2012). *Design of a Centrifugal Compressor.* Cape Town: Stellenbosch University.

Pope, J. (2009). *Analysis of a Turbocharger System for a Diesel Engine.* Hartford, Connecticut: Rensselaer Polytechnic Institute.

R.Flemming, F. L. (2011). *The Development of a High Speed Centrifugal Compressor Research Facility.* West Lafayette: Purdue University.

Schleer, M. W. (2006). *Flow Structure and Stability of a Turbocharger.* Zurich.

Sorokes, J. M. (2013). Selecting a Centrifugal Compressor. *Back to Basics*, 44-51.

8 APPENDICIES

8.1 Validation of Code

8.1.1 Geometry Code Validation

To validate the accuracy of the two Python codes, the geometry and compressor map of a Garrett compressor map were employed. The GT1548 model's dimensions and performance at the design point are outlined in *Table 11*. This compressor was chosen because its dimensions and performance were readily available. The actual impeller and the meridional view of its blades with dimensions are shown in *Figure 20*.

Table 11: GT1548 dimensions and performance at the design point

Feature	Dimension
Exducer radius	24mm
Inducer tip radius	18.6mm
Inducer hub radius	5.75mm
Pressure ratio at design point	1.625
Mass flow rate at design point	0.087kg/s
Efficiency at design point	72%
Number of blades (splitters)	6 (6)
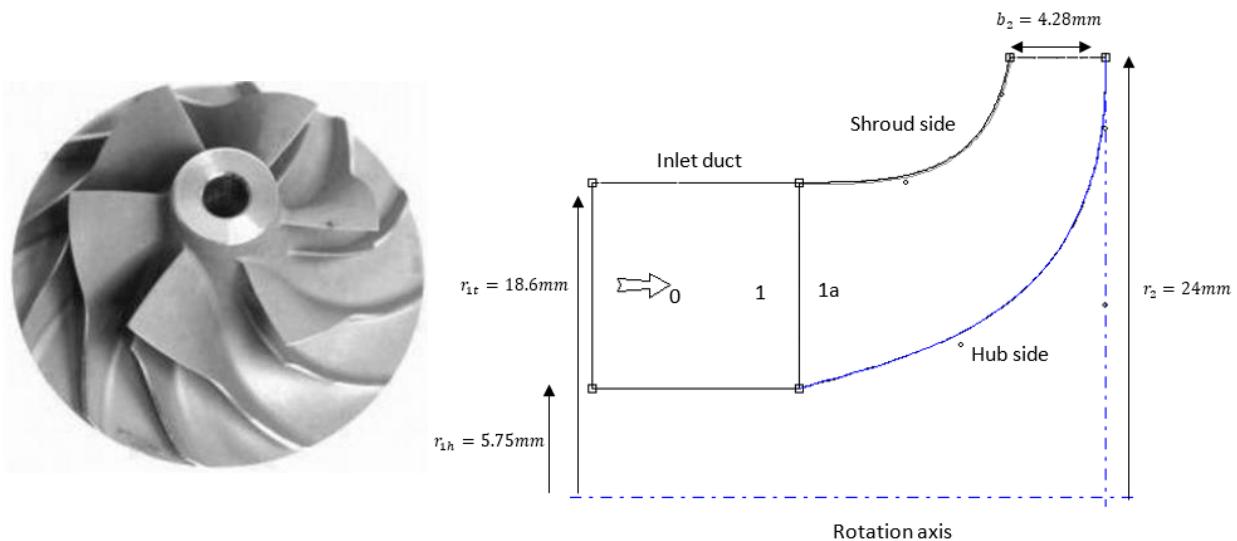
*Figure 20: Physical and meridional view of the GT1548 impeller with dimensions*

Table 12 compares the output dimensions and performance from the geometry code at the design point for the GT1548 compressor. The mass flow rate, radius of the hub, area ratio of the diffuser and the number of blades were inputs to the design code and thus were omitted from comparison of the values stated in *Table 11*.

Table 12: Validation of the design code based on the key dimensions and performance parameters

Feature	Dimension	Code Output	Error (-)	Error (%)
Exducer radius	24mm	24.18mm	0.18mm	**0.13%**
Inducer tip radius	18.6mm	15.61mm	3.01mm	**17%**
Pressure ratio at design point	1.62	1.57	0.05	**3%**
Efficiency at design point	0.72	0.67	0.05	**7%**

The 1-Dimensional mean line code provided an accurate description of a commercially manufactured centrifugal compressor. The errors observed for the exducer radius, pressure ratio and efficiency are likely the result of estimating empirical values used for the boundary layer blockage, B_1 and swirl parameter, λ_{2m}. The boundary layer blockage was chosen based on recommendation of Japikse (1996) who provides different empirical values for varying inlet duct shapes leading into the inducer. For both the validation and final design the inlet duct was taken to be axial and a value of 0.04 was selected. The exit swirl parameter was based on optimised vaneless diffusion behaviour for high speed, backswept impellers (Japikse, 1996). This value was chosen to be 2. The area ratio of the vaneless diffuser was not available and thus it was selected based of measurements of a similar sized compressor.

The calculation of the inducer under predicted its true size by 17%. The large error in the inducer is likely the result of Garrett designing the inlet tip to be larger than necessary to ensure that choke occurs in the diffuser rather than the inducer at high RPM. The large tip radius allows more mass flow for the same inlet speed which increases the operating range of the compressor but decreases pressure ratio. This is important in turbocharger design, which need to operate at high efficiency over a large range (Japikse, 1996).

The accuracy of the model for a 1-Dimensional geometry code was deemed valid based on this analysis. The code was found to determine the geometry to within an accurate tolerance for a given set of inputs. This validation meant that it could be used to design the geometry to meet the requirements of the application. Secondary flow calculations could improve the accuracy of code presented here. These calculations however are more appropriately used in applications where designs must be optimised for better efficiency. This was not a key requirement for this application, and thus it was deemed unnecessary to do.

8.1.2 Performance Code Validation

The performance code was validated by comparing the lines of constant speed for 120893, 153026 and 180046RPM from the GT1548 compressor map with those calculated by the off-design code. The accuracy of the code to determine the efficiency for different mass flows was also evaluated. The compressor map of the GT1548 is shown in *Figure 21* below.
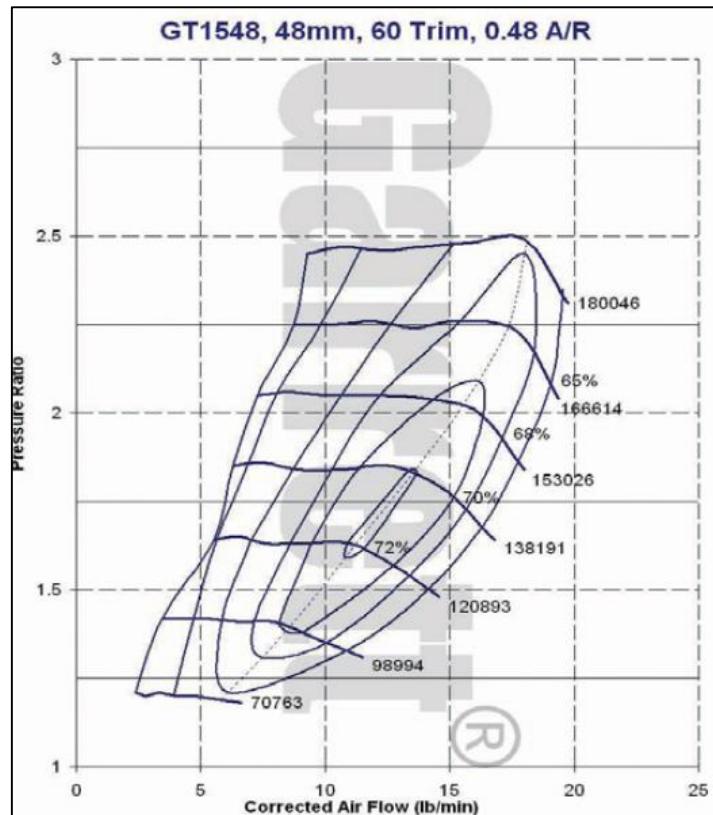
Figure 21: Compressor map of the GT1548

A comparison of the predicted and actual pressure ratios between surge and choke mass flow rates for each speed is shown in *Figure 22*. The surge and choke mass flow rates were determined by the approximate points of which the efficiency began to drop rapidly away from the peak of around 72%.
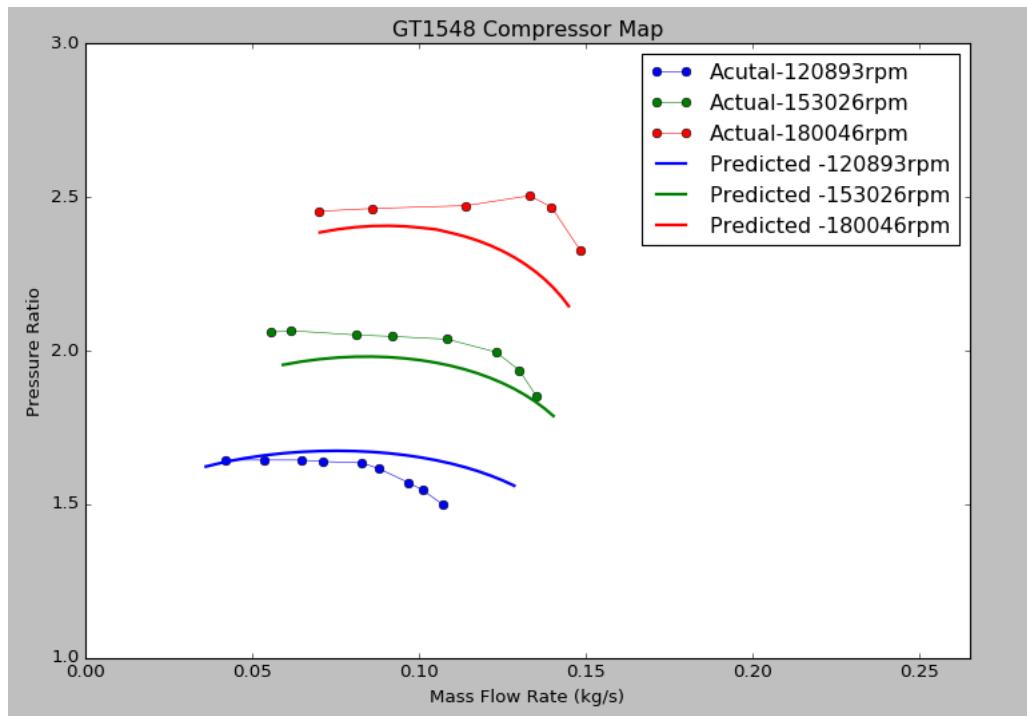

Figure 22: Compressor map comparison between the GT1548 and off-design performance code

The pressure ratio predictions were within a 10% accuracy for all mass flows. The surge and choke point predictions were determined with greater accuracy away from the design speed of 120893RPM. The slight errors in the code are likely due to the following points shown in order of the most significant.

- **Errors in the geometry calculation:** the increased inlet tip radius results in a higher root-mean-square static pressure calculation at the inducer. The pressure at the exit of the impeller is dependent on this pressure and consequently so is the overall pressure ratio. Furthermore, detailed geometry such as the blade curvature at the inlet and exact blade thickness were not available and hence were chosen based on best estimates.

- **Assumption of constant static pressure recovery in the diffuser:** To simplify the calculations, the assumption of constant static pressure recovery in the diffuser was made for all operating points. Typically, the static pressure recovery changes moderately over the operating range.

- **Empirical values:** On top of the empirical values used to establish the geometry of the compressor, the off-design uses a coefficient of friction and an estimate of the efficiency in the diffuser stage of the calculations. The coefficient of friction was taken from empirical data of other studies presented by Japikse and Baines (1997). The estimate of efficiency was recommended by QGECE. Furthermore, errors in the geometry code empirical inputs were likely to propagate into the design performance and have an impact on the accuracy of the model.

The predicted contours of efficiency as compared with those taken from the compressor map is shown in *Figure 23* for the same operating speeds used to compare the pressure ratios. The efficiencies predicted by the off-design code was found to be higher than those obtained experimentally by Garrett. The largest error was calculated to be at the peak efficiency at the highest speed, which was less than 5 percentage points. The mass flow rate corresponding to the peak efficiency was accurately predicted by the code, as was the general shape of the efficiency curve. The number of efficiency points for the actual measurements were limited which produced jagged points for the actual contours. The slight errors in the efficiency prediction are due to the same errors discussed above for the pressure ratio.
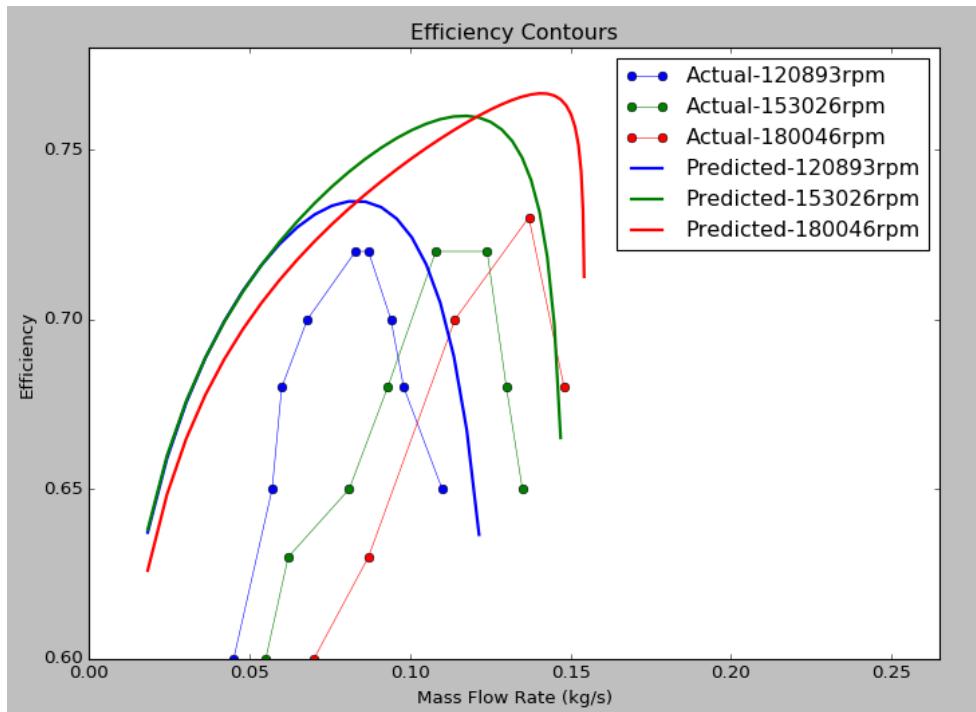
Figure 23: Efficiency contour comparison between the GT1548 and off-design performance code

Based on the assessment of the pressure ratio and efficiency, the models used to predict the geometry and performance of a centrifugal compressor for a given application were deemed valid. There are several limitations to the model which were found in this assessment and others noted by Galvas (1973)

- Both the geometry and performance codes are sensitive to the empirical values that are used. The empirical values are chosen based on literature and best estimates because they are not published by the manufacturer which limits the robustness of the code.

- The model assumes that the static pressure recovery in the diffuser is constant for all operating points. This does not occur in actual compressor, hence, it is a limitation of the model.

- The equations used to calculate slip are based on geometric parameters only, however the slip may vary substantially for each speed contour (Japikse, 1996).

- The off design performance code does not take into account shock losses

Overall, with the limitations considered, the geometry and off-design codes were validated against a commercially available compressor and thus could be used to design a centrifugal compressor for a given application.

8.2 Variable temperature and pressure code

The following script was used to calculate the lines of constant power, the effect of controlling inlet conditions and the plot of the 100kW line of constant power with mass flow rate in kg/s on the x-axis for *Figure 9 and Figure 10*. This code was also used to recreate the HE351Ve compressor map. Each section of the code was enabled and disabled by using three quotation marks ("""") on the top and bottom of the required section. For example, when plotting the varying pressure over the Holset compressor map, the requirement lines plot, variable temperature and the standardised mass flow rate sections were all disabled.

```
import numpy as np
import matplotlib.pyplot as plt
plt.close('all')

#Variables-------------------------------------------------------------------
comp_power=[20,100]         #Compressor power [kW]
speed=[120]                 #Shaft Speed [krpm]
T1=298                      #Inlet stagnation temperature [K]
cp=1.005                    #Specific heat at constant pressure [kJ]
y=1.4                       #Ratio of specific heats
P=0.1                       #Inlet pressure [MPa]
eta=0.75                    #Assumed efficiency

#Equation [8] ---------------------------------------------------------------
def pressure_ratio(mfp,eta,comp_power,P,T1,y,cp):
        return (eta*comp_power/(mfp*cp*P*T1**.5)+1)**(y/(y-1))

#Requirement lines plot------------------------------------------------------
mfp=np.arange(0,160,0.5)
plt.figure()
plt.xlim(0,160)
plt.ylim(1,5.0)
for i in range(2):
        Pr=pressure_ratio(mfp,eta,comp_power[i],P,T1,y,cp)
        plt.plot(mfp,Pr)
plt.legend(('20kW','100kW' ))
plt.show()

#Calculate variable temperature ---------------------------------------------
T0=[298,323,348,600]
for i in range (4):
        Pr=pressure_ratio(mfp,eta,100,P,T1[i],y,cp)
        plt.plot(mfp, Pr)
plt.xlim(0,140)
plt.ylim(1,5.0)
plt.xlabel('Mass Flow Parameter(MFP)', fontsize=15)
plt.ylabel('Total to Total pressure ratio', fontsize=15)
plt.title('Variable Inlet Temperature', fontsize=20)
plt.legend(('298K','323K','348K', '600K'))
```

```
plt.show()

#Calculate variable pressure ------------------------------------------------
P=[0.1,0.125,0.15,0.175]
for i in range (4):
        Pr=pressure_ratio(mfp,eta,100,P[i],T1,y,cp)
        plt.plot(mfp, Pr)
plt.xlim(0,140)
plt.ylim(1,5.0)
plt.legend(('0.1MPa','0.125MPa','0.15MPa','0.175MPa'))
plt.xlabel('Mass Flow Parameter(MFP)', fontsize=15)
plt.ylabel('Total to Total pressure ratio', fontsize=15)
plt.title('Variable Inlet Pressure', fontsize=20)
plt.show()

#Plotting mass flow rate in kg/s on x axis --------------------------------------
def pressure_ratio1(mdot,eta,comp_power,P,T1,y,cp)
return (eta*comp_power/(mdot*cp*T1)+1)**(y/(y-1))
mdot=np.arange(0,1.4,0.05)
plt.figure()
plt.xlim(0,1.4)
plt.ylim(1,5.0)
for i in range(1):
        Pr=pressure_ratio1(mdot,eta,comp_power[i],P,T1,y,cp)
        plt.plot(mdot,Pr, 'g-',linewidth=2)
plt.show()

#Plotting Holset HE351Ve compressor map -----------------------------------------------
plt.plot([25.10948472,31.16982327,38.02921278,44.41023875,51.27211801,57.499736],
[2.101782025,2.074240887,2.000797853,1.927354818,1.789649129,1.560139647],'k-o',
[36.71872019,43.89559601,51.55154674,59.68870643,67.19089349,74.22467601],
[2.900475022,2.863753505,2.808671229,2.680145919,2.478177575,2.019158611],
'k-o',[52.15024017,56.93529829,62.99670388,69.21969805,75.44696036,80.90113623],
[3.81851295,3.781791433,3.726709157,3.616544606,3.396215503,2.55162061],
'k-o',[13.01192671,18.59319036,23.8569677,28.96129053,33.90651452,39.65078947],
[1.560139647,1.550959268,1.505057372,1.459155475,1.4040732,1.303089027],
'k-o',[56.90506563,62.00796574,68.38685764,73.4922475,79.5600553,85.18435604],
[4.562123672,4.552943293,4.534582534,4.4611395,4.240810397,3.120804125],
'k-o',[12.69337336,24.79093137,36.55926568,51.51277779,56.74561111],
[1.550959268,2.092601646,2.900475022,3.809332571,4.562123672],
'k-o',[39.49133496,57.34028149,74.22467601,80.90078055,85.02419017],
[1.303089027,1.560139647,2.019158611,2.560800989,3.139164883],'k-o')
plt.annotate('126.86 RPS/K', xy=(56.74561111,4.562123672), xytext=(50 ,4.7), fontsize=15)
plt.annotate('114.17 RPS/K', xy=(51.51277779,3.809332571), xytext=(38 ,4),fontsize=15)
plt.annotate('97.58 RPS/K', xy=(36.55926568,2.900475022), xytext=(27 ,3),fontsize=15)
plt.annotate('78.07 RPS/K', xy=(24.79093137,2.092601646), xytext=(15 ,2.2),fontsize=15)
plt.annotate('58.55 RPS/K', xy=(12.69337336,1.550959268), xytext=(10 ,1.25),fontsize=15)
plt.show()
```

8.3 Geometry Code

'''

The following code takes a set of variables as inputs and calculates the geometry of an inducer, impeller and diffuser for a centrifugal compressor.
'''

```python
'Mitchell Lowe, 21/8/2016'
import math
import numpy as np
import matplotlib.pyplot as plt


###Variables-----------------------------------------------------------------------------------


P00=101300                  #Inlet stagnation pressure [Pa]
T00=293                     #Inlet stagnation temperature [K]
mdot=0.4                    #Mass flow rate [kg/s]
Ndes=120000                 #Rotational speed [rpm]
alpha1=0                    #Absolute inlet velocity angle [degrees]
rh1=0.01                    #Hub radius [mm]
B1=0.04                     #Boundary layer blockage [-]
Cp=1005                     #Specific heat at constant pressure [kJ/kg/K]
k=1.4                       #Ratio of specific heats [-]
R=287                        #Air gas constant [J/kg/K]
Cm1i=np.arange(100,300.5,0.5) #Absolute meridional velocity [m/s]
Pr=4.8                      #Pressure ratio [-]
lambda2=2                   #Exit swirl parameter
beta2b=-40                  #Exit relative direction [degrees]
eta=0.6                     #Stage efficiency [-]
ZB=16                       #Number of Blades [-]
AR=2.5                      #Area ratio of the diffuser [-]
T00i=np.full(len(Cm1i),293) #Inlet stagnation temperature [K]
D2=0.105                    #Chosen exit diameter [m]


###Inducer calculation-------------------------------------------------------------------------


Ctheta1i=Cm1i*math.tan(math.radians(alpha1)) #Inlet absolute tangential velocity [degrees]
C1i=(Ctheta1i**2 + Cm1i**2)**0.5        #Absolute velocity [m/s]
T1i=T00i-(C1i**2)/(2*Cp)                #Inlet temperature [K]
M1i=C1i/((k*R*T1i)**0.5)                #Inlet Mach number [-]
P1i=P00*(T1i/T00)**(k/(k-1))            #Inlet pressure [Pa]
rho1i=P1i/(R*T1i)                       #Inlet density of air [kg/m^3]
A1i=mdot/(rho1i*Cm1i*(1-B1))            #Inlet flow area [m^2]
#rt1i=(A1i/(math.pi*(1-(hubtip)**2)))**0.5 #Inlet tip radius [m]
rt1i=(A1i/math.pi +rh1**2)**0.5         #Inlet tip radius [m]
U1ti=2*math.pi*rt1i*Ndes/60            #Inlet blade tip speed [m/s]
W1ti=(Cm1i**2 +((U1ti**2)-(Ctheta1i**2)))**0.5 #Inlet relative velocity [m/s]

Ctheta1=Ctheta1i[np.argmin(W1ti)]
C1=C1i[np.argmin(W1ti)]
T1=T1i[np.argmin(W1ti)]
M1=M1i[np.argmin(W1ti)]
```

```
P1=P1i[np.argmin(W1ti)]
rho1=rho1i[np.argmin(W1ti)]
A1=A1i[np.argmin(W1ti)]
rt1=rt1i[np.argmin(W1ti)]
U1t=U1ti[np.argmin(W1ti)]
W1t=W1ti[np.argmin(W1ti)]
Cm1=Cm1i[np.argmin(W1ti)]
beta1= math.degrees(math.atan((U1t-Ctheta1)/Cm1)) #Inlet relative velocity [degrees]

def W1tminimise(Cm1i, U1ti,Ctheta1i):
        return (Cm1i**2 +((U1ti**2)-(Ctheta1i**2)))**0.5
        W1tmin=W1tminimise(Cm1i, U1ti,Ctheta1i)
plt.figure()
plt.plot(Cm1i, W1tmin)
plt.xlabel("Cm1(m/s)")
plt.ylabel("W1t(m/s)")
plt.title("Minimisation of W1t")
plt.show()


###Impeller calculation-------------------------------------------------------------------------

sigma=1-(math.sqrt(math.cos(math.radians(beta2b)))/(ZB**0.7)) #Slip factor [-]
mu=sigma*lambda2/(lambda2-math.tan(math.radians(beta2b))) #Work input coefficient [-]
hx=((k*R*T00)/(k-1))*(Pr**((k-1)/k) -1)     #Specific enthalpy [kJ/kg/K]
Wx=hx/eta                                   #Specific work [kJ/kg/K]
T02m=T00+Wx*(k-1)/(k*R)                      #Stagnation exit temperature [K]
P02m=P00*(((k-1)*Wx*eta/(k*R*T00))+1)**(k/(k-1)) #Exit Stagnation Pressure [Pa]
#U2=((U1t*Ctheta1+Wx)/mu)**0.5               #Exit Blade Speed [m/s]
#D2=60*U2/(math.pi*Ndes)                      #Exit Diameter [m]
U2=D2*math.pi*Ndes/60                         #Exit blade speed [m]
Ctheta2m=mu*U2                               #Absolute tangential exit velocity [m/s]
Cm2m=Ctheta2m/lambda2                        #Absolute meridional exit velocity [m/s]
T2m=T02m-(k-1)/(2*k*R)*(Ctheta2m**2+Cm2m**2) #Exit temperature [K]
P2m=P02m/((T02m/T2m)**(k/(k-1)))             #Exit pressure [Pa]
rho2m=P2m/(T2m*R)                            #Exit density [kg/m^3]
A2=mdot/(rho2m*Cm2m)                         #Exit area [m^2]
b2=A2/(math.pi*D2)                           #Depth of impeller exit [m]
C2=(Ctheta2m**2+Cm2m**2)**0.5                #Absolute exit velocity [m/s]


###Diffuser Calculation-------------------------------------------------------------------------

etad=0.85                 #Estimated diffuser efficiency
CpDi=1-(AR**-2)           #Ideal pressure recovery coefficient
CpD=etad*CpDi             #Pressure recovery coefficient
P3=P2m+CpD*(P02m-P2m)     #Diffuser exit static pressure [Pa]
C3=C2/AR                  #Diffuser exit absolute velocity [m/s]
P03=P3+0.5*rho2m*C3**2    #Diffuser exit stagnation pressure [Pa]


###Overall performance-------------------------------------------------------------------------
etaiterate=((P03/P00)**((k-1)/k)-1)/((T02m/T00)-1)              #Iterative stage efficiency [-]
```

```
Prest=((etaiterate*U2**2*mu)/(Cp*T1)+1)**(k/(k-1))        #Estimate of the pressure ratio

###Code Outputs-------------------------------------------------------------------------------------
print "Pressure ratio=", P03/P00
print "Pressure ratio error=", Pr-P03/P00
print "Efficiency=", etaiterate
print "Efficiency error=", abs(etaiterate-eta)
print "Work=", Wx*mdot, "Watts"
print "Mass flow rate=", mdot, "kg/s"
print "Exducer diameter=", D2*1000, "mm"
print "Inducer Diameter=", rt1*2000, "mm"
print "Exit blade speed=", U2
if rt1/(0.5*D2) < math.exp(-8.16*math.cos(beta2b)/ZB):      #Check for sigma validity
        print "sigma valid"
else:
        print "sigma invalid!"
```

8.4 Off-design Code

Note that the letter B and number inside the brackets in some of the lines of code correspond to the equations in NASA's Fortran model (B46, B47...B60 for example). The B denotes Appendix B in the original paper and the number corresponds to the equation number in approximate order of use in the code (Galvas, 1973). There is a jump in numbers between B7-B40 and B72-B84. The missing equations correspond to inlet guide vane losses and vaned diffuser losses, both of which were omitted for reasons outlined in *Section 4*.2. Many of the variables and equations used in this code have not been defined in this thesis. The full set of equations and a description of the calculation process can be found in Appendix B of NASA's Fortran model. A description of each calculation line in the code is provided after the hash symbol (#). Additionally, a description of each function that has been used is also provided.

```
'''
The following code uses the inducer and impeller geometry from the geometry code
(FinalDesignCode) and predicts the performance of the compressor at off-design points
'''
'Mitchell Lowe, 21/8/2016'
from FinalDesignCode import*
import math
import numpy as np
import matplotlib.pyplot as plt


###Variables-------------------------------------------------------------------------------------------

Ndes=120000
No=1.0                  #Off design speed percentage that requires performance prediction [rpm]
tu=0.002                #Blade thickness [m]
rho0=1.1839             #Stagnation density of air [kg/m^3]
curvet1=0               #Inducer inlet tip wall curvature [m^-1]
curveh1=0               #Inducer inlet hub wall curvature [m^-1]
x=10                    #Streamline angle [degrees] from axial direction
VCR=math.sqrt(2*k/(k+1)*R*T00) #Critical Velocity [m/s]
VOVCR=np.arange(0.1,0.8,0.025) #Compressor inlet absolute critical velocity ratio [-]
Cm1h=VOVCR*VCR          #Absolute meridional velocity of the hub [m/s]
kBL=0.6                 #Blading loss coefficient [-]
visc=1.778e-5           #Air viscosity based on total conditions
kSF=7.0                 #Skin friction coefficient [-]
Cf=0.01                 #Friction coefficient [-]
T00i=np.full(len(VOVCR),293)

###Calculation of Inlet Velocity Triangles and Compressor Weight Flow (Swirl free)---------

curve1rms=math.sqrt((curvet1**2+curveh1**2)/2) #Root mean square of the inducer inlet
hub and tip wall curvature [m^-1]
r1rms=math.sqrt((rt1**2 +rh1**2)/2) #Root mean square of the hub and tip inlet radius [m]
```

h0=r1rms-rh1   #(B4) Spacing for numerical integration [-]
h1=rt1-r1rms   #(B5) Spacing for numerical integration [-]
Cm1rms=Cm1h*math.exp((h0/2)*(curveh1+curve1rms)) #(B2)Absolute meridional root mean square velocity [m/s]
Cm1t=Cm1h*math.exp(((h0+h1)/6)*((2-(h1/h0))*curveh1+(((h0+h1)**2)/(h1*h0))*curve1rms+(2-(h0/h1))*curvet1)) #(B3)Absolute meridional velocity of the tip [m/s]
Cm1hn=Cm1h*math.cos(math.radians(x)) #(B6) Normal component of the absolute hub velocity [m/s]
Cm1tn=Cm1t*math.cos(math.radians(x)) #(B6) Normal component of the absolute tip velocity [m/s]
Cm1rmsn=Cm1rms*math.cos(math.radians(x)) #(B6) Normal component of the root mean square velocity [m/s]
rho1h=rho0*(1-(Cm1h**2/(2*Cp*T00)))**(1/(k-1)) #Inlet density of the air at the hub [kg/m^3]
rho1rms=rho0*(1-(Cm1rms**2/(2*Cp*T00)))**(1/(k -1)) #Root mean square density of the air [kg/m^2]
rho1t=rho0*(1-(Cm1t**2/(2*Cp*T00)))**(1/(k-1)) #Inlet density of the air at the blade tip [kg/m^3]
mdoto=2*math.pi*(((h0+h1)/6) *((2-(h1/h0))*(rho1h*rh1*Cm1hn)+((h0+h1)**2/(h0*h1))*(rho1rms*r1rms*Cm1rmsn)+(2-(h0/h1))*(rho1t*rt1*Cm1tn)))   #(B7)Off Design point mass flow rate [kg/s]
U1to=math.pi*No*Ndes*2*rt1/60   #Off design blade tip velocity [m/s]
U1ho=math.pi*No*Ndes*2*rh1/60   #Off design blade hub velocity [m/s]
U1rmso= ((U1to**2+U1ho**2)/2)**0.5   #Off design rms velocity [m/s]
W1ho=(Cm1h**2+U1ho**2)**0.5   #Off design hub relative velocity [m/s]
W1to=(Cm1t**2+U1to**2)**0.5   #Off design tip relative velocity [m/s]
W1rmso=((W1ho**2+W1to**2)/2)**0.5   #rms relative velocity [m/s]
beta1t=[]
beta1h=[]
beta1rms=[]
T1=T00i-(Cm1rms**2)/(2*Cp) #Inlet static temperature [K]
for i in range (0, len(VOVCR)):
        beta1t.append(math.degrees(math.atan(Cm1t[i]/U1to))) #Hub inlet relative angle [degrees]
        beta1h.append(math.degrees(math.atan(Cm1h[i]/U1ho))) #Tip inlet relative angle [degrees]
        beta1rms.append(((beta1t[i]**2+beta1h[i]**2)/2)**0.5) #rms inlet relative angle [degrees]

###Inducer Incidence Loss--

BBF=1-(ZB*tu)/(2*math.pi*r1rms) #(41)Blade Blockage Factor [-]
eps=[]
betaopt=[]
WL=[]
dhinc=[]
T1orel=[]
WCR=[]
W1rmseff=[]

```
T0T1=[]
T1a=[]
T1rmso=[]
P1rmso=[]
P1arms=[]
for i in range(0,len(VOVCR)):
        eps.append(math.degrees(math.atan((1-
        BBF)*math.tan(math.radians(beta1rms[i]))/(1+BBF*math.tan(math.radians(beta1rms
        [i]))**2)))) #(B40)Difference between compressor inlet relative flow angle and
        optimum incidence angle [degrees]
        betaopt.append(beta1rms[i]-eps[i]) #(B42)Optimum relative flow angle [degrees]
        WL.append(W1rmso[i]*math.sin(math.radians(abs(betaopt[i]-beta1rms[i]))))
        #(B43)Component of relative velocity lost [m/s]
        dhinc.append((WL[i]**2)/(2*Cp)) #(B44)Enthalpy loss due to incidence [J/kg]
        T1orel.append(T1[i]+W1rmso[i]**2/(2*Cp)) #Off design inlet relative temperature
        [K]
        WCR.append((2*(k-1)/(k+1)*R*T1orel[i])**0.5) #Critical inlet relative velocity
        [m/s]
        W1rmseff.append(W1rmso[i]*math.cos(betaopt[i]-beta1rms[i])) #Effective relative
        velocity [m/s]
        T0T1.append(1-(k-1)/(k+1)*(W1rmseff[i]/WCR[i])**2) #Ratio of inlet static
        temperatures [-]
        T1a.append(T1orel[i]*T0T1[i]) #Temperature just inside the blade [K]
        T1rmso.append(T00i[i]-(Cm1rms[i]**2/(2*Cp))) #Off design Root mean square of
        static temperature at inlet [K]
        P1rmso.append(P00*(T1rmso[i]/T00i[i])**(k/(k-1))) #Off design root mean square of
        static pressure at the inlet [Pa]
        P1arms.append(P1rmso[i]*math.exp((-1*dhinc[i])/(T1a[i]*R))) #(B45)Total pressure
        just inside the bladed row [Pa]


###Impeller Work and Losses------------------------------------------------------------------------

U2o=U1to/(rt1/(D2/2))          #Off design exit blade velocity [m/s]
dhest=U2o**2                   #(B46) Initial approximation of enthalpy rise in impeller [J/kg]
T2oestabs=(dhest/(Cp*T00)+1)*T00 #(B47) Estimate of the off design impeller exit total
temperature [k]
rho2o=rho1*(T2oestabs/T00)**(1/(k-1)) #(B48) Off design impeller exit density [kg/m^3]
"""
The Densityiteration(rho2o) function takes an initial guess of the impeller outlet density using
Equation B48 above. It then uses this initial guess to calculate a series of velocities,
temperatures and enthalpies corresponding to this initial guess before re-calculating the
density.
"""
def Densityiteration(rho2o):
        Vm2m=mdoto/(math.pi*rho2o*D2*b2) #(B49) Meridional component of exit
        absolute velocity [m/s]
        VSL=U2o*(1-sigma) #(B51) Slip velocity [m/s]
        Vtheta2=(U2o-Vm2m*math.tan(math.radians(-beta2b))-VSL) #(B50) Tangential
        component of exit absolute velocity [m/s]
        T1orelrms=T1+W1rmso**2/(2*Cp) #Relative root mean square temperature [K]
```

T2orel=T1orelrms+((U2o**2-U1t**2)/(2*Cp)) #(B52) Exit temperature in the relative reference frame [k]
#T2orel=T1+((U2o**2-U1t**2)/(2*Cp))
Wtheta2=U2o-Vtheta2 #(B53) Tangential component of relative exit velocity [m/s]
W2=((Vm2m**2)+(Wtheta2**2))**0.5 #(B54) Relative exit velocity [m/s]
T2o=(T2orel-((W2**2)/(2*Cp))) #(B55) Off design point exit temperature [K]
V2=((Vm2m**2)+(Vtheta2**2))**0.5 #(B56) Off design point absolute exit velocity [m/s]
T2oabs=(T2o+(V2**2)/(2*Cp)) #(B57) Off design point exit temperature in the absolute reference frame [K]
dhaero=(Cp*T00*(T2oabs/T00-1)) #(B61) Aerodynamic enthalpy rise [J/kg]
qaero=dhaero/(U2o**2) #(B60) Dimensionless actual head [-]
Df=(1- W2/W1to +(kBL*qaero)/((W1to/U2)*((ZB/math.pi)*(1-2*rt1/D2)+2*2*rt1/D2))) #(B59)Diffusion factor [-]
dhBL=(0.05*Df**2*U2o**2) #(B58) Work loss due to blade loading [J/kg]
Re=U2o*D2*rho1rms/visc #(B63) Reynolds number of the exit flow [-]
dhDF=(0.01356*rho2o*U2o**3*D2**2/(mdoto*Re**0.2)) #(B62) Impeller disk friction loss [J/kg]
D1rms=math.sqrt(((((2*rt1)**2)+((2*rh1)**2))/2) #Rootmean square of the diameter [m]
Lendia=0.5*(1-(D1rms/0.3048))/(math.cos(math.radians(beta2b))) #(B65) Blade length to diameter ratio [-]
HYDdia= 1/(ZB/(math.pi*math.cos(math.radians(beta2b))+D2/b2))
+(2*rt1/D2)/(2/(1-k)+2*ZB/(math.pi*(1+k))*math.sqrt(1+(math.tan(math.radians(beta1)**2)*(1+k**2/2)))) #Ratio of hydraulic diameter and exit diameter [-]
WRelExt=0.5*((Cm1rms/U2o)**2+(D1rms/D2)**2+(W2/W1to)**2*((Cm1rms/U2o)**2+(2*rt1/D2)**2)) #(B67)Ratio of mean relative velocity and impeller exit velocity^2 [-]
dhSF=((kSF*Cf*Lendia*WRelExt*U2o**2)/HYDdia) #(B64) Skin Friction loss [J/kg]
dhid=(dhaero-dhinc-dhSF-dhDF-dhBL) #(B68) Ideal enthalpy rise [J/kg]
etaR= dhid/dhaero #(B69) Impeller efficiency [-]
P2oabs=(P1arms*(etaR*dhaero/(Cp*T00)+1)**(k/(k-1))) #(B70)Iteration of the off design exit absolute pressure [Pa]
P2o=(P2oabs/((T2oabs/T2o)**(k/(k-1)))) #(B71)Iteration of the off design exit pressure [Pa]
rho2oit=P2o/(R*T2o) #(B72) Iteration of the off design exit density [kg/m^3]
return
[rho2oit,T2o,dhaero,dhBL,dhDF,dhSF,dhid,T2oabs,P2oabs,Vtheta2,Vm2m,Df,P2o]
'''
The Density()function selects the value corresponding to the variables listed below when the output density from the DensityIteration(rho2o) function is within 0.1% of the input
'''
def Density():
        rhoinit=rho2o
        RHO=[]
        T2o=[]
        dhaero=[]
        dhBL=[]

```
        dhDF=[]
        dhSF=[]
        dhid=[]
        T2oabs=[]
        P2oabs=[]
        Vtheta2=[]
        Vm2m=[]
        Df=[]
        P2o=[]
        for i in range(0,len(VOVCR)):
                rhoafter=Densityiteration(rho2o)[0][i]
                rho=[rhoinit,rhoafter]
                while abs((rho[-1])-(rho[-2]))>0.00001:
                        if abs((rho[-1])-(rho[-2])) >0.001:
                                rho.append(Densityiteration(rho[-1])[0][i])
                        else:
                          if len(RHO)<i+1:
                                rho.append(Densityiteration(rho[-1])[0][i])
                                RHO.append(Densityiteration(rho[-1])[0][i])
                                T2o.append(Densityiteration(rho[-1])[1][i])
                                dhaero.append(Densityiteration(rho[-1])[2][i])
                                dhBL.append(Densityiteration(rho[-1])[3][i])
                                dhDF.append(Densityiteration(rho[-1])[4][i])
                                dhSF.append(Densityiteration(rho[-1])[5][i])
                                dhid.append(Densityiteration(rho[-1])[6][i] )
                                T2oabs.append(Densityiteration(rho[-1])[7][i])
                                P2oabs.append(Densityiteration(rho[-1])[8][i])
                                Vtheta2.append(Densityiteration(rho[-1])[9][i])
                                Vm2m.append(Densityiteration(rho[-1])[10][i])
                                Df.append(Densityiteration(rho[-1])[11][i])
                                P2o.append(Densityiteration(rho[-1])[12][i])
                          else:
                          rho.append(Densityiteration(rho[-1])[0][i])
                return [RHO,T2o,dhaero,dhBL, dhDF, dhSF, dhid, T2oabs, P2oabs, Vtheta2,
                Vm2m,Df,P2o]

rho2=np.array(Density()[0])
T2o=np.array(Density()[1])
dhaero=np.array(Density()[2])
dhBL=np.array(Density()[3])
dhDF=np.array(Density()[4])
dhSF=np.array(Density()[5])
dhid=np.array(Density()[6])
T2oabs=np.array(Density()[7])
P2oabs=np.array(Density()[8])
Vtheta2=np.array(Density()[9])
Vm2m=np.array(Density()[10])
Df=np.array(Density()[11])
P2o=np.array(Density()[12])
C2o=[]
```

```python
for i in range(0,len(VOVCR)):
        C2o.append((Vm2m[i]**2+Vtheta2[i]**2)**0.5)


###Recirculation Loss------------------------------------------------------------------------

dhRC=[]
alpha2=[]
for i in range(0,len(VOVCR)):
        alpha2.append(math.degrees(math.atan(Vtheta2[i]/Vm2m[i])) ) #Exit velocity flow
        angle [degrees]
        dhRC.append(0.02*math.sqrt(math.tan(math.radians(alpha2[i])))*Df[i]**2*U2o**2)
        #Enthalpy loss from recirculation [kJ/kg]


#Exit losses-----------------------------------------------------------------------------------

etad=0.85
CpDi=1-(AR**-2)
CpD=etad*CpDi
M3o=[]
P3oabs=[]
dhVLD=[]
P3o=[]
C3o=[]
P03o=[]
for i in range(0,len(VOVCR)):
        P3o.append(CpD*0.5*rho2[i]*(C2o[i])**2+P2o[i])
        C3o.append(C2o[i]/AR)
        P03o.append(P3o[i]+0.5*rho2[i]*C3o[i]**2)
        M3o.append(C3o[i]/(math.sqrt(k*R*T2oabs[i])))
        P3oabs.append(P3o[i]*(1+(k-1)/2*M3o[i]**2)**(k/(k-1))) #(B85) Absolute diffuser
        throat pressure [Pa]
        dhVLD.append(Cp*T2oabs[i]*((P3o[i]/P3oabs[i])**((k-1)/k)-
        (P3o[i]/P2oabs[i])**((k-1)/k))) #(B86)Vaneless diffuser loss [kJ/kg]
###Overall performance-------------------------------------------------------------------------

etao=[]
Pro=[]
for i in range(0,len(VOVCR)):
etao.append((dhaero[i]-
(dhinc[i]+dhBL[i]+dhSF[i]+dhVLD[i]))/(dhaero[i]+dhRC[i]+dhDF[i]))
Pro.append(P3o[i]/P00)
print "Mass flow rate=",mdoto
print "Pressure ratio=",Pro
print "Efficiency=",etao


plt.figure()
plt.plot(mdoto,etao,'b-')
plt.xlabel("Mass flow rate (kg/s)")
plt.ylabel("Efficiency (%)")
```

```
plt.title("Efficiency contour")
plt.xlim(0,1)
plt.show()
plt.figure()
plt.plot(mdoto,Pro,'r', label="120000RPM", linewidth=1.25)
plt.xlabel("Mass flow rate (kg/s)")
plt.ylabel("Pressure ratio(-)")
plt.title("Compressor Map")


###Matching------------------------------------------------------------------------------------

comp_power=[100] #Compressor power [kW]
speed=[120] #Shaft Speed [krpm]
T1=293 #Inlet stagnation temperature [K]
cp=1.005 #Specific heat at constant pressure [kJ]
y=1.4 #Ratio of specific heats
P=0.1013 #Inlet pressure [MPa]
eta=0.6 #Assumed efficiency


###Line of constant power-------------------------------------------------------------
def pressure_ratio1(mdot,eta,comp_power,P,T1,y,cp):
        return (eta*comp_power/(mdot*cp*T1)+1)**(y/(y-1))
mdot=np.arange(0,1.4,0.025)
plt.xlim(0,0.6)
plt.ylim(1,8)
for i in range(1):
        Pr=pressure_ratio1(mdot,eta,comp_power[i],P,T1,y,cp)
plt.plot(mdot,Pr, 'g-', label="100kW", linewidth=1.25)
plt.show()
plt.legend()
```